CHAPTER IV

DIELECTRIC STUDIES ON SEVERAL STRUCTURALLY RELATED SMECTOGENIC COMPOUNDS

4.1 Introduction

Dielectric properties of liquid crystals have been the subject of numerous studies since the beginning of the century. Maier and Meier[1] were the first to systematically measure the principal dielectric constants of di-alkoxy substituted azo and azoxy benzenes. Since then, there have been many studies to relate the dielectric properties with the molecular structure. (For a summary, see de Jeu.[2])

Many liquid crystals with strong positive dielectric anisotropy have bean synthesized and their properties investigated[3,4] after the discovery of twisted nematic effect by Schadt and Helfrich.[5] More recently, as we have already discussed in the previous chapters, the study of liquid crystals composed of strongly polar molecules led to the discovery of two interesting phenomena: re-entrance[6-8] and smectic A polymorphism.[9] The liquid crystalline phases of these compounds are, generally speaking, characterized by bilayer structures which are

a consequence of interactions between permanent dipoles ail the molecules.[10] Dielectric studies are important in understanding the nature of intermolecular interactions. Hence, measurements of static dielectric constants were taken up in the smectic, nematic and isotropic phases of several structurally related smectogenic compounds, the Xray studies on which were discussed in the previous chapter. The transition temperatures of the compounds studied are listed in table 4.1. Dielectric relaxation studies (up to 13 MHz) were also made on a few compounds. [Dielectric studies were taken up only on compounds which were available in sufficient quantities.] The results are presented and discussed in this chapter.

(i) Static dielectric constants

Nematic and smectic A phases are optically uniaxial and hence possess two dielectric constants: $\varepsilon_{\parallel}$ parallel to the director and $\varepsilon_{\perp}$ in a perpendicular direction. The sign and magnitude of the dielectric anisotropy ($\Delta\varepsilon = \varepsilon_{\parallel} - \varepsilon_{\perp}$) depend upon tho permanent dipole moments and polarisabilities of the molecules. For rod like molecules, the polarisability anisotropy ($\Delta\alpha = \alpha_{\parallel} - \alpha_{\perp}$) la always positive. Hence, in the absence of permanent dipolar groups the dielectric anisotropy is positive and relatively small.

On the other hand, the dielectric anisotropy of polar compounds depends upon the sign of the dipolar contribution. It fa positive if the net dipole moment μ of the molecule makes a small angle with the long axis and is negative if the angle made by a sufficiently strong μ is large. Liquid crystals with both the signs and a large range of values of $\Delta\varepsilon$ have been synthesized.

A semi-quantitative explanation of these widely varying dielectric properties was given by Maier and Meier[11] who extended Onsager's[12] theory of polar liquids to nematics using the molecular field approximation.[13]

Maier and Meier's theory gives the following expressions for the dielectric constants

$$\varepsilon_{\parallel} = 1 + 4\pi N h F \left\{ \bar{\alpha} + \frac{2}{3}\Delta\alpha S + \frac{F\mu^2}{3k_B T}[1 - (1 - 3\cos^2\beta)S] \right\} \quad .. \quad (4.1)$$

$$\varepsilon_{\perp} = 1 + 4\pi N h F \left\{ \bar{\alpha} - \frac{1}{3}\Delta\alpha S + \frac{F\mu^2}{3k_B T}[1 + \tfrac{1}{2}(1 - 3\cos^2\beta)S] \right\} \quad .. \quad (4.2)$$

where $\Delta\alpha$ is the anisotropy of polarizability of a perfectly oriented medium, $\bar{\alpha}$ the mean polarizability, β the angle made By the permanent dipole moment μ with the long molecular axis, S the orientational order parameter, N the number @$ molecules per unit volume, $h = 3\bar{\varepsilon}/(2\bar{\varepsilon}+1)$ the cavity field factor, $F = 1/(1 - \bar{\alpha}f)$,

$f = (4\pi N/3)[(2\bar{\varepsilon}-2)/(2\bar{\varepsilon}+1)]$ the reaction field factor and K_B the Boltzmann constant. We get for the anisotropy of the dielectric constant,

$$\Delta\varepsilon = \varepsilon_{\parallel} - \varepsilon_{\perp} = 4\pi N h f \left\{ \Delta\alpha - \frac{\mu^2}{2K_B T}(1 - 3\cos^2\beta) \right\} S \qquad (4.3)$$

The widely varying dielectric properties of the nematics can be understood qualitatively on the basis of this equation. The relative magnitudes of the two terms within the flower brackets of the equation (4.3) determine the sign of $\Delta\varepsilon$, when β is smaller than $\simeq 55°$, the two terms add up and the compound has a strong positive dielectric anisotropy. For $\beta \simeq 55°$, the second term vanishes and only $\Delta\alpha$ contributes to $\Delta\varepsilon$. For higher values of β $\Delta\varepsilon > 0$ or < 0, depending upon whether the dipolar contribution is less or more than the contribution due to polarisability anisotropy. More interestingly, if the two terms within the flower brackets in equation (4.3) are practically equal, it is clear that $\Delta\varepsilon$ can change sign at some temperature T, and become negative at lower temperatures as is indeed found in some systems.[14]

From (4.1) and (4.2) we can calculate the mean dielectric constant ($\bar{\varepsilon}$) In the nematic phase,

$$\bar{\varepsilon} = \left(\frac{\varepsilon_{\parallel} + 2\varepsilon_{\perp}}{3}\right) = 1 + 4\pi NhF\left(\bar{\alpha} + \frac{\mu^2}{3k_B T}\right) \qquad (4.4)$$

The dielectric constant in the isotropic phase can be obtained by substituting $S = 0$ in either (4.1) or (4.2)

$$\varepsilon_{is} = 1 + 4\pi NhF\left(\bar{\alpha} + \frac{\mu^2}{3k_B T}\right) \qquad (4.5)$$

As the density change and hence the change in N at T_{NI} is very small ($\sim 0.5\%$) equations (4.4) and (4.5) imply that $\bar{\varepsilon}$ value should practically coincide with ε_{is} at T_{NI}. But $\bar{\varepsilon}$ is found to coincide with ε_{is} only for nonpolar mesogens like p-p'-di-n-alkylazobenzenes.[15] On the other hand, a noticeable positive jump in $\bar{\varepsilon}$ value has been observed in several strongly polar compounds.[3,4] The difference can be as high as 4-5%.[4,16] Also, $\bar{\varepsilon}$ is found to decrease with decrease of temperature in such strongly polar compounds.[3,4] Maier and Meier's theory fails to account for these observations. The main drawback of the theory is that it neglects short range order effects in the medium.

As discussed in chapter III, Madhusudana and Chandrasekhar[17] have proposed that in such compounds the neighbouring molecules have antiparallel correlations. They included an antiparallel short range order term in the interaction potential and using it in the Maier and

Meier's theory of dielectric anisotropy, showed theoretically that $\bar{\varepsilon}$ in the nematic phase should be less than the extrapolated value from the isotropic phase. me theoretical curve is reproduced in fig.4.1. The positive jump in the value of $\bar{\varepsilon}$ observed at T_{NI} is interpreted aa due to a discontinuous decrease in the antiparallel correlations between neighbouring molecules. The decrease of $\bar{\varepsilon}$ with decrease of temperature is evidently due to the increase in the antiparallel ordering at lower temperatures.

(ii) Dielectric relaxation

It is well known that dielectric constants are frequency dependent. In the nematic and smectic phases, the relaxation of $\varepsilon_\perp$ corresponding to reorientation about the long molecular axis, occurs in the GHz region while relaxation of $\varepsilon_\parallel$, arising from molecular reorientations about the short molecular axis, occurs in MHz or sometimes even in KHz region. This difference in frequency dependences of $\varepsilon_\parallel$ and $\varepsilon_\perp$ can be easily understood on the basis of the fact that all liquid crystals possess orientational order and hence the molecular reorientations about the short axis of the rod like molecule will be strongly hindered. The low frequency relaxation of

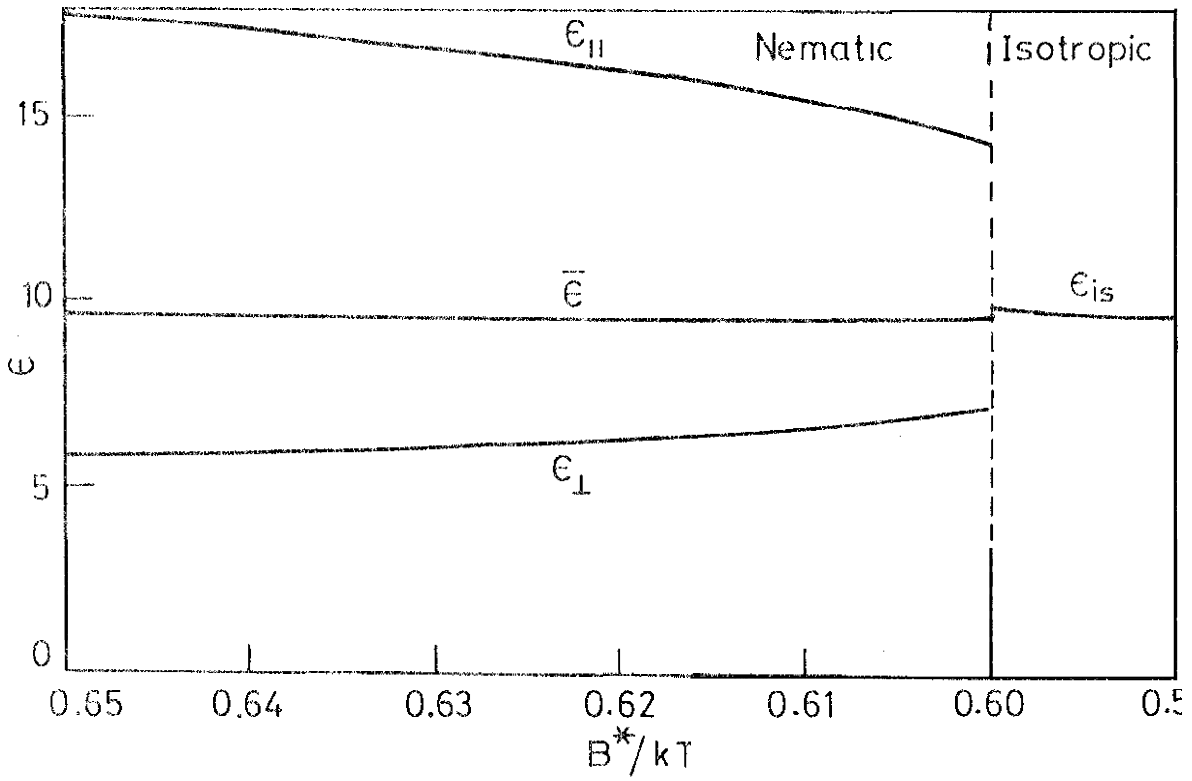

FIGURE 4.1

Theoretical variation of the dielectric constants $\epsilon_{\parallel}$, $\epsilon_{\perp}$, ϵ_{is} and $\bar{\epsilon} = (\epsilon_{\parallel} + 2\epsilon_{\perp})/3$ evaluated for $A^*/B^* = 0.5$ (Reproduced from ref.17).

$\epsilon_{\parallel}$ was first observed by Maier and Meier[18] in several members of the p-azoxyanisole (PAA) series. They correctly attributed it to the effect of the nematic potential.

The dipole moment μ of a molecule making an angle θ with the long molecular axis has components $\mu_l = \mu\cos\theta$ in the longitudinal direction and $\mu_t = \mu\sin\theta$ in the transverse direction. The reorientation of μ_l is hindered by the nematic order resulting in a low frequency relaxation of $\epsilon_{\parallel}$. On the other hand, μ_t can reorient more easily about the long axis and correspondingly $\epsilon_{\perp}$ relaxes usually In the GHz or la some cases in 10 - 100 MHz region. As the orientational order in the medium f a less than one, μ_t also contributes to the relaxation of $\epsilon_{\parallel}$, leading to a second relaxation of $\epsilon_{\parallel}$ in the high frequency (LO MHz - GHz) region.

Meier and Saupe and later Martin at al.[19] extended the Debye[20] model of dielectric relaxation in liquids to nematics. They defined a retardation factor $g = \tau_R/\tau_0$ where τ_R is the observed relaxation time of $\epsilon_{\parallel}$ in the nematic phase and τ_0 the ordinary Debye relaxation time in the isotropic phase. Assuming that the molecule has only the longitudinal component of the dipole moment, they were able 60 relate the retardation factor for $\epsilon_{\parallel}$

with the nematic potential (q). The relationship between g and q is given by the expression

$$g = \frac{k_B T}{q}[\exp(q/k_B T) - 1] \simeq \frac{k_B T}{q} \exp(q/k_B T)$$

In the isotropic phase, the hindrance to the molecular reorientations is mainly due to the viscosity of the medium. The temperature dependence sf the viscosity is expressed as $\eta \propto \exp[q_\eta/k_B T]$, where q_η is the activation energy due to viscosity effects and in the isotropic phase $\tau_0 \propto \eta/k_B T$. From the definition of the retardation factor we have, $\tau_R = g\tau_0$ and hence

$$\tau_R \propto \exp[(q + q_\eta)/k_B T]$$

Therefore, $w = q + q_\eta$ is the total activation energy for dielectric relaxation in the nematic phase. The relaxation frequency $f_R = 1/2\pi\tau_R$ and hence $f_R \propto \exp(-w/k_B T)$. A plot of $\ln f_R$ vs. $1/T$ should give a straight line, the slope of which gives the activation energy w. Thus the activation energy can be determined by measuring f_R of $\varepsilon_{\parallel}$ at various temperatures.

The frequency dependence of the dielectric constant means that $\varepsilon_{\parallel}$ is actually complex and is given by $\varepsilon_{\parallel} = \varepsilon'_{\parallel} + i\varepsilon''_{\parallel}$ where the real part $\varepsilon'_{\parallel}$ describes the ordinary dielectric constant and the imaginary part $\varepsilon''_{\parallel}$ the

losses associated with the relaxation processes.

Cole and Cole[21] suggested a graphical representation (now called the Cole-Cole plot) which indicates the nature of relaxation. It in obtained by plotting the experimental values of $\varepsilon''(\omega)$ against those of $\varepsilon'(\omega)$. Per the case of single relaxation time, ε' and ε'' are given by

$$\varepsilon'(\omega) = \varepsilon_{\infty} + \frac{\varepsilon - \varepsilon_{\infty}}{1 + \omega^2\tau^2}, \quad \varepsilon''(\omega) = \frac{(\varepsilon - \varepsilon_{\infty})\omega\tau}{1 + \omega^2\tau^2}$$

and the points $(\varepsilon', \varepsilon'')$ lie on a semicircle with the centre an the ε' axis and intersecting this at $\varepsilon' = \varepsilon$ and $\varepsilon' = \varepsilon_{\infty}$ where ε and ε_{∞} are the static and high frequency dielectric constants. Deviations from the semicircle *plot* indicate a distribution of relaxation times.

Earlier observations on nematic and smectic A liquid crystals show that the Cole-Cole plot is usually a semicircle in the case of $\varepsilon_{\parallel}$ relaxation while it is not so in the case of $\varepsilon_{\perp}$ indicating a distribution *of* relaxation frequencies in the latter case.[22]

4.2 Experimental

(i) Materials

All the compounds studied were synthesised in our chemistry laboratory.[23,24] The transition temperatures and heats of transition are listed in table 4.1. The structural formulae along with the acronyms are given in fig.4.2.

(ii) Heater

A schematic diagram of the heater is shown in fig.4.3a. The heater consisted of a copper rod having a rectangular slot along its length. Nichrome heater wires were wound at both the ends (CC) of the heater to avoid temperature gradients in the sample. Glass windows (W) were provided at the centre to make visual observations of the sample alignment. The heater could be rotated about a vertical axis and its position could be read on a circular scale(S) attached to its bottom to an accuracy of 0.1°. This enables us to make both $\epsilon_{\parallel}$ and $\epsilon_{\perp}$ measurements on the same sample by rotating the sample by 90°. The heater is mounted on a stand between Me pole pieces (NS) of a strong electromagnet. The current supply to the heater is drawn from a stabilized source (Digireg 165).

Table 4.1

Transition temperatures (in °C) and enthalpies (in KJ/mole) of the compounds studied

Compound	K	A_2	A_d	N	I
12 PMCBB	• [67.5] [16.8]	• 77.1	• [155.3] [0.42]	• [159.3] [1.48]	•

Compound	K	A	N	I
9 PMNBB	• 75.9 [16.3]	(• 66.1) [0.019]	• 156.5 [1.11]	•
10 PMNBB	• 77 [21.6]	• 108.5 [0.062]	• 150.0 [1.13]	•
12 PMNBB	• 73.3 [20.0]	• 141.3 [0.165]	• 146.9 [1.28]	•
10 PMeOCBB	• 97.8 [33.7]	(• 94)	• 135.4 [1.56]	•
11 PMeOCBB	• 105 [35.1]	• 122 [0.035]	• 136 [1.8]	•
11 CPMeOBB	• 121 [41.2]	• 130.1 [0.17]	• 133.3 [1.6]	•
12 CPMeOBB	• 122.8 [43.5]	• 131.7	• 132.2 [3.13]	•
11 PMeOBrBB	• 102.5	(• 85.3) [0.26]	(• 95.6) [1.46]	•

Numbers in square brackets indicate enthalpies in KJ/mole.
( ) indicate monotropic transitions.

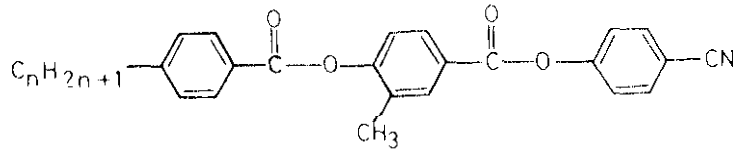

4 - cyanophenyl - **3 - methyl - 4'-(4''** - n - alkyl benzoyloxy) benzoates

(nCPMBB)

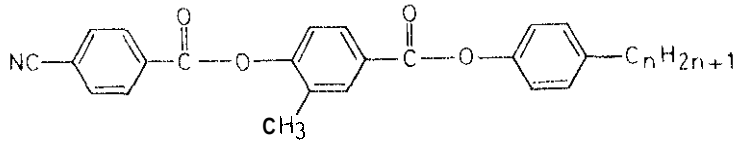

4 - n - alkylphenyl - 3 - methyl - 4'- (4''-cyanobenzoyloxy) benzoates

(nPMCBB)

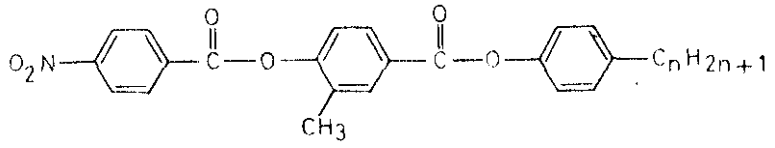

4 - n - alkylphenyl **- 3 -** methyl - 4'- (4''- nitrobenzoyloxy) benzoates

(nPMNBB)

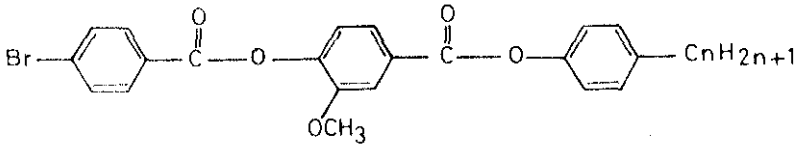

4 - n - alkylphenyl - **3' - melhoxy - 4'** - (4''- bromobenzoyloxy) **benzoates**

(nPMeOBrBB)

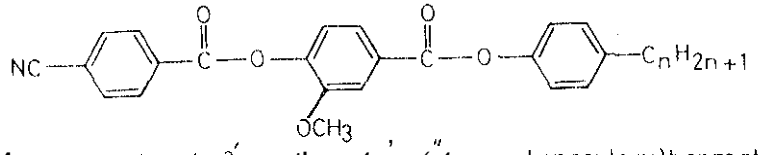

4 - n - alkylphenyl - 3'- **rnethoxy** 4' - (''4 cyanobenzoyloxy) benzoates

(nPMeoCBB)

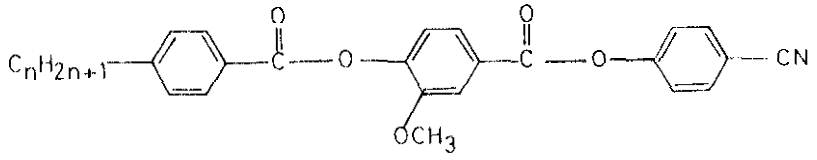

4 - cyanophenyl - 3'- methoxy - 4'- (4''- n - alkyl benzoyloxy) benzoates

(nCPMeOBB)

FIGURE 4.2: Structural formulae and acronyms of various compounds used in our studies,

(iii) Dielectric Cell

The dielectric constants were determined by measuring the capacitance of a parallel plate capacitor without and with the sample. The schematic diagram of the dielectric cell used in shown in fig.4.3b. The cell consisted of two tin oxide coated plates (O) which served as electrodes. They were separated by mylar spacers (M) of thickness 100 - 125 μm. Care was taken to ensure that the mylar spacers were outside the active area. The two electrodes were offset along their lengths and connected to copper leads (L) via platinum foils (P) which ensure good electrical contact. The cell was held rigidly in a copper frame (F) using screws S_1 and S_2 as shown in fig.4.3b. The frame could be inserted into the heater such that the cell was positioned at the centre of the heater and magnetic pole pieces and held in place by means of four brass screws. The cell holder had provisions for evacuation of the system (through the nozzle N) and insertion of a thermocouple (T).

(iv) Temperature measurement

The temperature of the sample was measured using a calibrated copper-constantan thermocouple (T) and a Keithley 174 digital multimeter. The temperature of the sample could be maintained to an accuracy of $\pm 0.1^{o}$C over long periods.

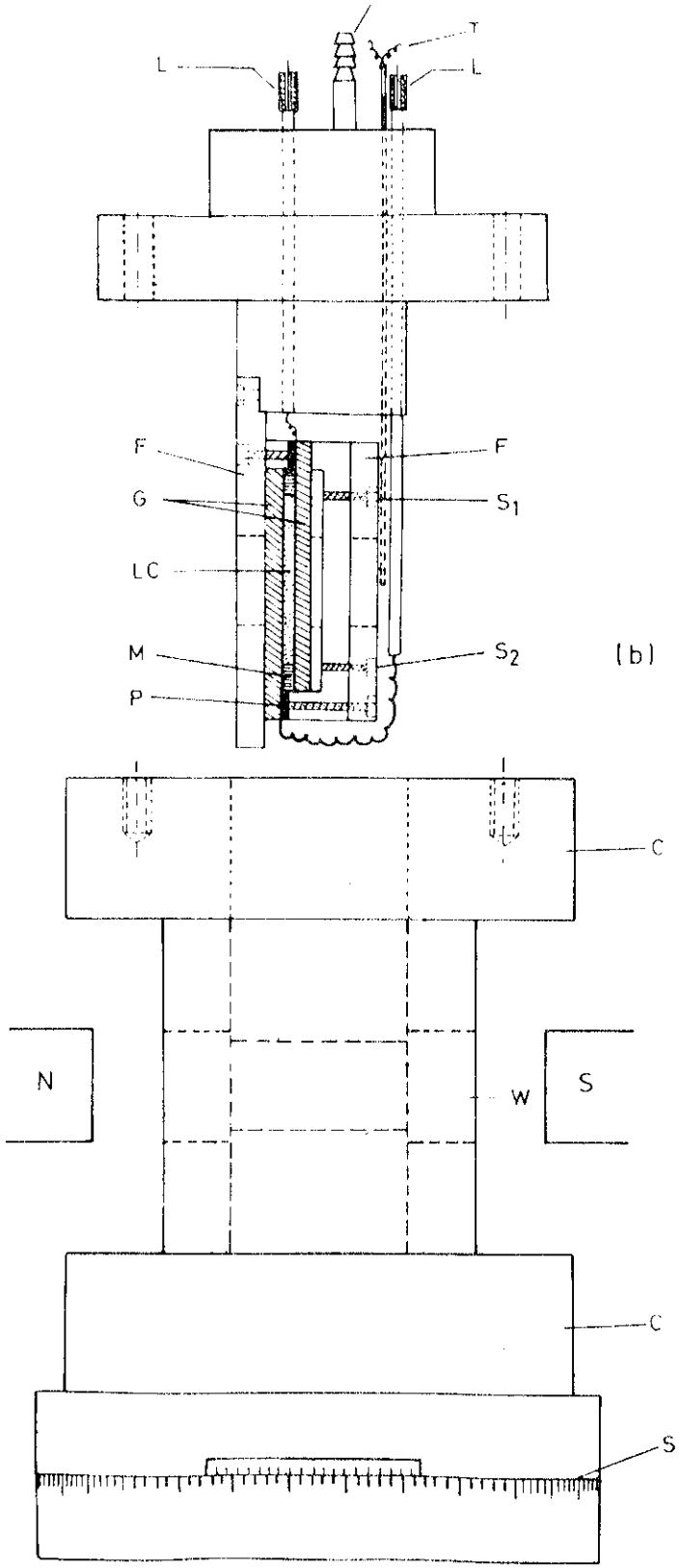
T
L
L
F
F
G
S_1
LC
M
S_2
P
(b)
C
N
W
S
C
S

FIGURE 4.3

Schematic diagram of (a) Heater (b) dielectric aell.

C - Circular parts over which the heater is wound

W - Window for the visual observation of the sample.

NS - Pole pieces of a permanent magnet

S - Circular scale

M - Mylar spacers

P - Platinum foil

LC - Liquid Crystal

G - Glass plates

F - Metal frame

S_1 & S_2 - Screws used for holding the glass plates in position

L - Lead wires (shielded)

T - Copper-Constanton thermocouple

N - Nozzle.

(v) Measurement of static dielectric constants

As the sample alignment is known to be affected by surface conditions, the electrodes were cleaned thoroughly first with a detergent (Teepol) and then with freshly prepared chromic acid. The plates were dipped in a dilute solution of sodium bicarbonate to remove any acid trace and then thoroughly washed with distilled water.

The cell was calibrated using standard organic liquids (benzene, toluene and chlorobenzene). The values obtained for these liquids always agreed with the standard values within 1% which is therefore considered to be the absolute accuracy of our measurements.

The cell was filled with the sample while it was in the nematic phase. The cell was then inserted into the heater assembly which was evacuated and then filled with nitrogen. Care was taken to ensure that there were no air bubbles in the sample.

A magnetic field of strength $\simeq$ 14 KGauss was used for the sample alignment. For the measurement of $\varepsilon_{\parallel}$, the sample was aligned homeotropically and the electric field was applied along the director ($\vec{E} \parallel \vec{n}$). $\varepsilon_{\perp}$ was measured by aligning the sample homogeneously

and applying the electric field perpendicular to the director ($\vec{E} \perp \vec{n}$). In the absence of the magnetic field the director vaires from point to point and the measured dielectric constant has a value between the two principal dielectric constants. As the magnetic field is increased, the measured values of $\varepsilon_{\parallel}$ and $\varepsilon_{\perp}$ change until 'saturation' values are reached when the orientation is uniform throughout the sample. This saturation test was made in a22 our measurements. A field strength of $\simeq$14 KGauss was found to yield saturation values in all the compounds studied.

The low frequency dielectric constants were measured by using a Wayne Kerr bridge, model B642, at a frequency of 1592 Ha. The capacitances were measured to an accuracy better than 0.1% and hence this could be taken as the accuracy la the relative variation of $\varepsilon_{\parallel}$ and $\varepsilon_{\perp}$ values. The measured capacitance was always corrected for the lead capacitance.

Measurements of the principal dielectric constants were made in the isotropic, nematic and smectic A phases. The alignment in the smectic A phase was obtained by slowly cooling the sample from the nematic to the smectic A phase in the presence of the magnetic field.

(vi) Dielectric relaxation studies

The experimental set up was the same as that used in static measurements. However, the tin oxide coated plates could not be used because of the high losses involved. Instead aluminium coated glass plates wan used.

The dispersion was measured up to 13 MHz using Hew2886 Packard LF impedance analyser (Model 4192A). The measured capacitances and conductances were corrected for lead inductance. For each compound, the real and imaginary parts of both $\varepsilon_{\parallel}$ and $\varepsilon_{\perp}$ were measured at various temperatures. The temperature was stabilised at the desired value for at least half-an-hour before taking measurements. In order to check our experimental set up for dispersion measurements, we carried out studies on n-heptylcyanobiphenyl (7CB). Our experimental results were in agreement with the earlier data available in the literature.[22,25]

$\varepsilon_{\parallel}$ relaxed in the measured frequency range for all the compounds studied while a broad relaxation of $\varepsilon_{\perp}$ was observed in the compound 4-n-undecylphenyl-3'-methoxy-4'-(4"-cyanobenzoyloxy)benzoate (11 PMeOCBB).

4.3 Results and Discussion

(A) Static dielectric constants

The principal dielectric constants $\varepsilon_{\parallel}$ and $\varepsilon_{\perp}$, the average value $\bar{\varepsilon}$, isotropic value ε_{is} and the dielectric anisotropy ($\Delta\varepsilon$) are shown in figure 4.4 for 12 PMOBB. The salient features are (a) $\varepsilon_{\parallel}$ increases with the decrease of temperature in the nematic phase but starts decreasing fairly rapidly as the temperature is lowered in the smectic A phase. The rate of decrease goes down at lower temperatures; (b) $\varepsilon_{\perp}$ has exactly the opposite trend though the rate of variation is somewhat smaller than that of $\varepsilon_{\parallel}$; (a) the two curves cross at $T_{NI} - T \simeq 40°C$ so that $\Delta\varepsilon$ changes sign from positive to negative at that temperature; d) $\bar{\varepsilon}$ increases as the temperature is lowered in the isotropic phase and decreases in the mesophases. The variation of $\bar{\varepsilon}$ appears to show a cusp at T_{NI}, the nematic-isotropic transition temperature.

These interesting results can be understood as follows. We have shown the significant dipole moments of various bonds (taken from Ref.26) of an nPMOBB molecule in fig. 4.5. The conformation all the molecule is not known but the three phenyl rings are very unlikely to

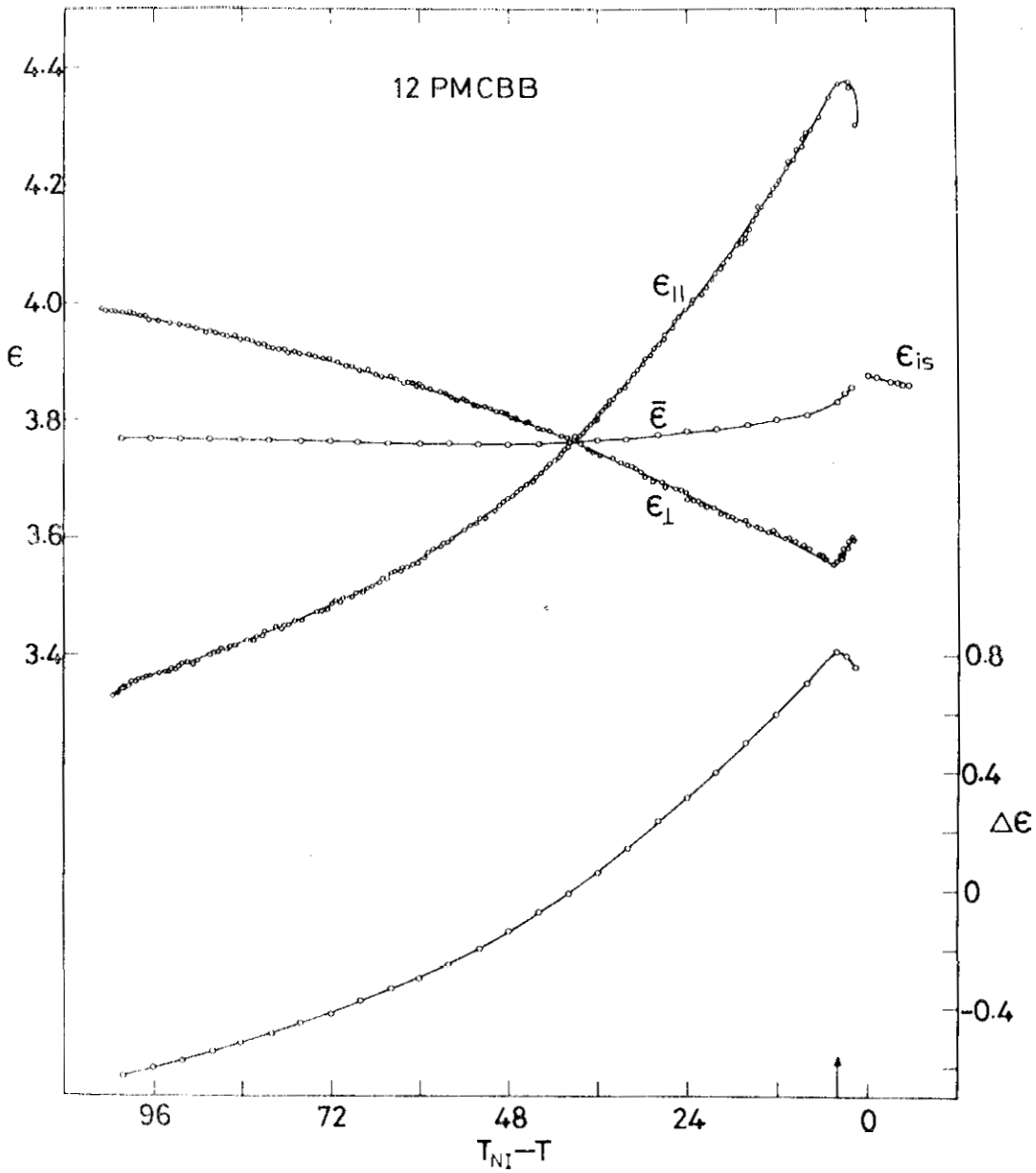

FIG.4.4: Temperature variations of the low frequency dielectric constants (upper part) and the dielectric anisotropy (lower part) of 12 PMCBB measured at 1592 Hz. $T_{NI} - T$ is the relative temperature, T_{NI} being the nematic-isotropic transition temperature. The arrow mark indicates the nematic-smectic A transition point (T_{AN}).

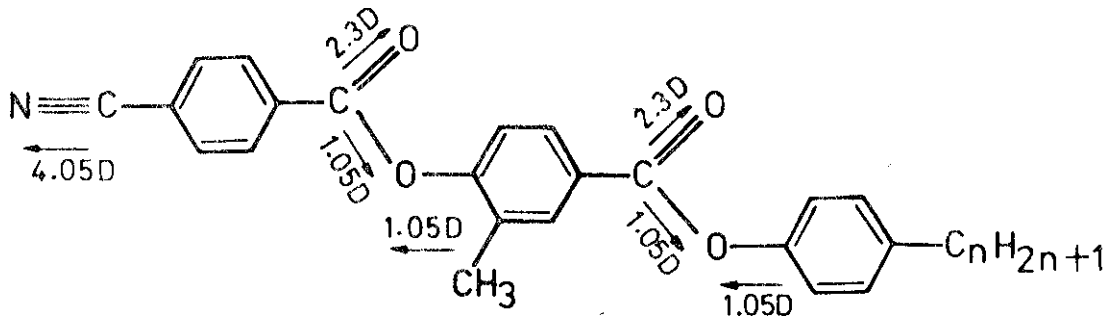

(n PMCBB)

FIGURE 4.5

The most important dipole moments of different groups of an n-PMCBB molecule (taken from referenoe 26)

of
be coplanar. The values $\mu_{\perp}$ and $\mu_{\parallel}$, the components paralleland perpendicular to the long axis of the net dipole μ depend on the molecular conformation. From eqn.(4.3), we see that $\Delta\epsilon \propto \{\Delta\alpha - (N\mu^2/2k_BT)(1 - 3\cos^2\beta)\}S$ and if the two terms within the flower brackets are of similar magnitude, the dielectric anisotropy can be very small and can even change sign at some temperatures becoming positive at higher temperatures. Thus Maier and Meier's theory predicts the reversal of $\Delta\epsilon$ in the N phase which has been indeed observed in some systems.[14] This mechanism could indeed be contributing to the reversal of the sign of $\Delta\epsilon$ in 12 PMCSB also, but we must note some additional points: if it is the only mechanism, $\bar{\epsilon}$ should have decreased with increase of temperature (see eqn.4.4). $\bar{\epsilon}$ actually varies in the opposite manner, which could be attributed to an increasing antiparallel short range order between neighbouring molecules at lower temperatures.[17] In addition, the reversal occurs in the A phase which has a layered structure. Benguigui[27] has shown that in such a case, the dipole correlation factors *far* $\mu_{\perp}$ and $\mu_{\parallel}$ will be such as to lower $\epsilon_{\parallel}$ and enhance $\epsilon_{\perp}$.

We get a natural explanation for the observed temperature variation of $\bar{\epsilon}$ on the basis of the model

proposed in chapter III to understand the thermal variation of bilayer spacings in nPMCBB and other similar compounds. The model showing the interdigitation in the bilayer is shown *in* fig.4.6. In nPMCBB compounds an overlap of the aromatic cores (4.6b) would result la strong repulsive interactions between the dipole moment of the cyano group of one molecule and that of one of the ester groups of the other. The dipolar aontribution to the interaction energy would be minimum when the overlap occurred only near the cyano end groups as shown in fig. 4.6c. Thus, as the temperature is lowered, more and more number 45 molecules form antiparallel associations as shown in fig. 4.6c (for a detailed discussion see chapter III). This leads to an enormous expansion of the layer spacing with the lowering of temperature. This mechanism accounts for the dielectric properties α' 12 PMCBB also. At lower temperatures, a large number of molecules are associated in pairs near the cyano group and the contribution of the dipole moment of the cyano end group to the polarizability is more effectively reduced. This gives rise to a faster reduction of $\varepsilon_{\parallel}$ as the %@we- rature is lowered, compared to the increase of $\varepsilon_{\perp}$ predicted by eqn.(4.2). Thus $\bar{\varepsilon}$ decreases with decrease of tempe-

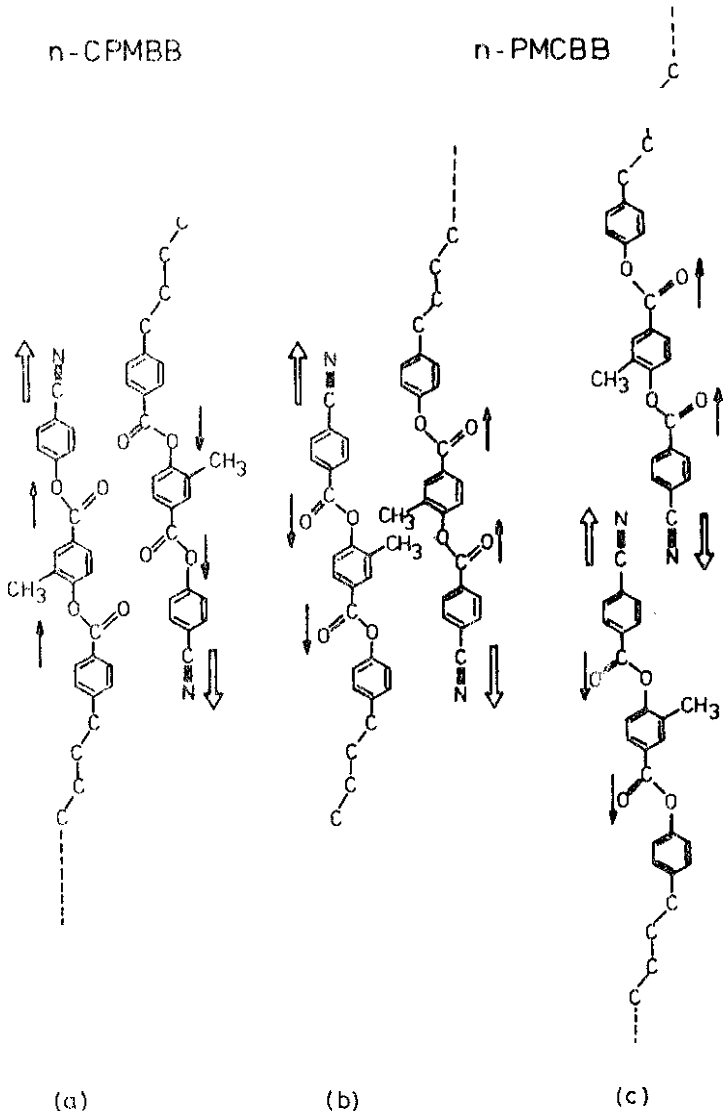

FIG.4.6: Schematic diagrams showing the disposition of various dipolar groups of a pair of (a) n-CPMBB, (b) n-PMCBB molecules with an overlap of the aromatic cores, and (c) a pair. of n-PMCBB molecules with an overlap of the polar end groups.

rature. These trends in $\varepsilon_{\parallel}$ and $\varepsilon_{\perp}$ variations lead to the reversal of $\Delta\varepsilon$.

We make a further remark regarding the increase of $\varepsilon_{\perp}$ with decrease of temperature. As we will see later, the relaxation of $\varepsilon_{\perp}$ in the case of related compound 11 PMeOCBB indicates that the pairs associated near the cyano groups reorient as a single unit under the action of the external AC field acting perpendicular to the long axis. If the dipolar groups contributing to μ_t of the two molecules in the pair are favourably oriented, the polarization of the medium perpendicular to the long axis can increase due to the pair formation. In this case, as the temperature is lowered, the number of such pairs increases leading to an increase of $\varepsilon_{\perp}$. The reversal of the temperature variations of both $\varepsilon_{\parallel}$ and $\varepsilon_{\perp}$ in the A phase compared to those in the N phase shows the important influence of layering and the variation of its structure on the dielectric properties of these compounds.

The dielectric properties of 10 PMeOCBB and 11 PMeOCBB are shown in figs.4.7 and 4.8 respectively. In both the compounds, $\varepsilon_{\parallel}$ increases as the temperature is decreased from T_{NI}. It attains a maximum, which is

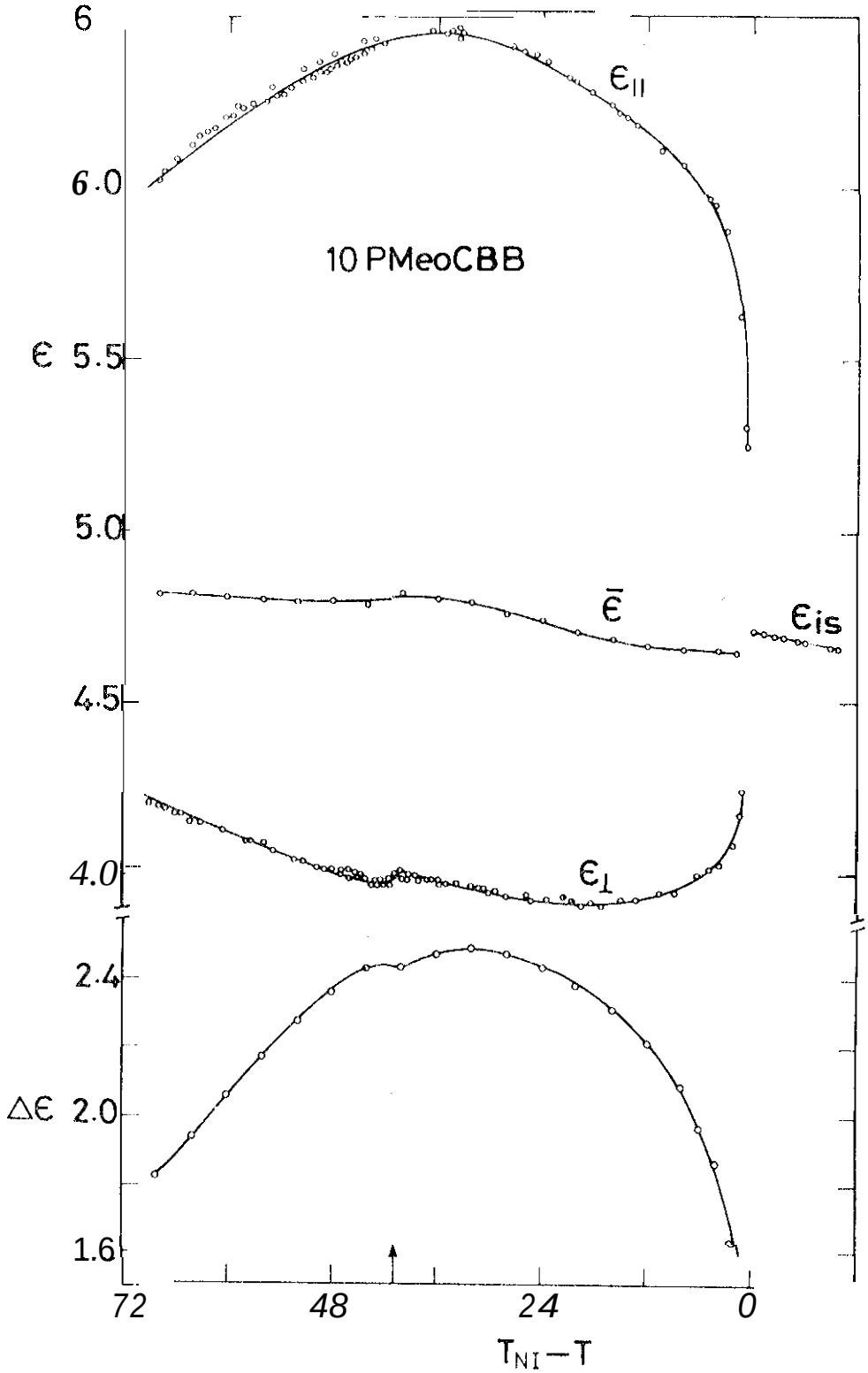

FIG.4.7: Temperature variations of the low frequency dielectric constants (upper part) and anisotropy (lower part) of 10 PMeOCBB measured at 1592 Hz. The arrow mark indicates T_{AN}.

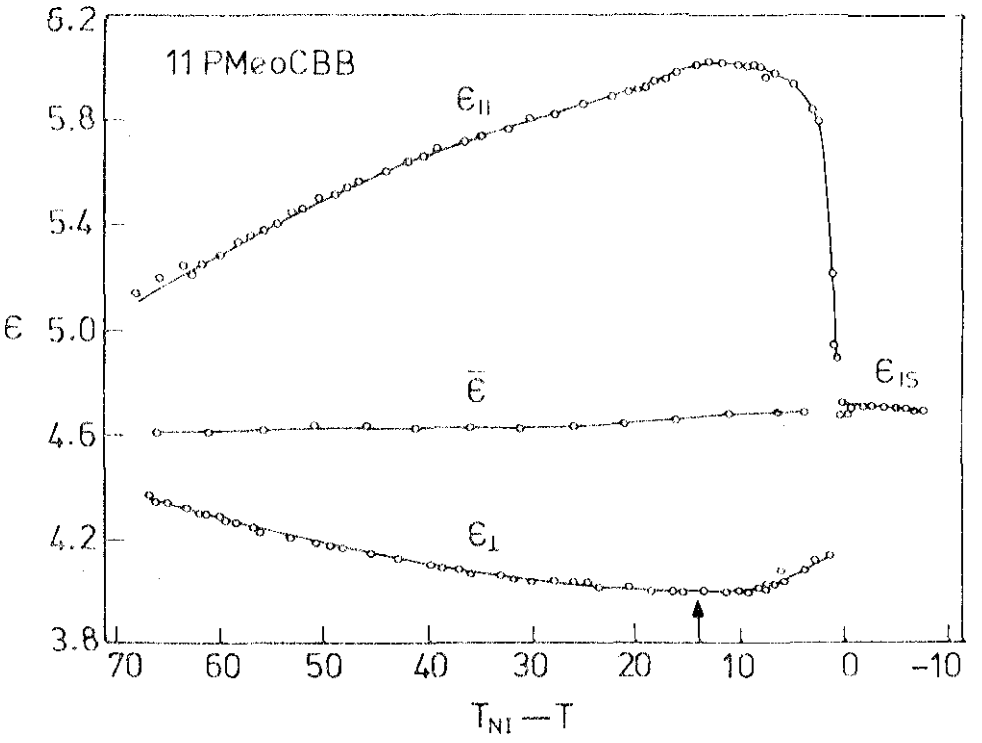

FIGURE *4.8*

Temperature variations of the low frequency dielectric constants of 11 PMeOCBB measured at 1592 Hz. The arrow mark indicates T_{AN}.

slightly broader in 10 PMeOCBB, a few degrees above T_{AN} and then continuously decreases in the A phase. This means that smectic like short range order effects are felt a few degrees above T_{AN}, since the corresponding heat of transition is quite small in both the compounds (see table4.1). The decrease of $\varepsilon_{\parallel}$ in 11 PMeOCBB is much greater than that in 10 PMeOCBB. This is due to the much larger range of temperature over which the A phase is stable In 11 PMeOCBB. In 10 PMeOCBB, as temperature is lowered $\varepsilon_{\perp}$ starts increasing at a relatively high temperature in the N phase, and shows a small cusp like peak at T_{AN}. This may be caused by the misalignment close to T_{AN} which is also observed in some other compounds that favour a homeotropic alignment[28] close to T_{AN}. In 11 PMeOCBB, $\varepsilon_{\perp}$ decreases with decrease of temperature in the N phase, attains a broad minimum close to T_{AN} and then continuously increases in the A phase with lowering of temperature. No cusp like peak is observed in this case indicating a better alignment. In both the cases, $\bar{\varepsilon}$ shows a positive jump at T_{NI} and decreases slightly as the temperature is increased in the isotropic phases. $\bar{\varepsilon}$ shows a slight increasing trend in the tenth member while it remains practically constant in the eleventh homologue with decrease of temperature in the liquid crystalline phases. $\varepsilon_{\parallel}$, $\varepsilon_{\perp}$

and $\bar{\varepsilon}$ have somewhat higher values in nPMeOCBB than in the case of 12 PMCBB because of the additional oxygen atom which has a high polarizability.

The dielectric constants of 9 PMNBB, 10 PMNBB and 12 PMNBB (nitro analogues of nPMCBB compounds) are shown in figs.4.9-4.11. The dielectric properties of 9 PMNBB (fig.4.9) are broadly similar to those of 10 PMeOCBB (fig.4.7). As the temperature is lowered, $\varepsilon_\perp$ starts increasing at a fairly high temperature far above T_{AN}. $\varepsilon_\parallel$ starts decreasing at a somewhat lower temperature, though still above T_{AN}. The decrease of $\varepsilon_\parallel$ becomes very rapid at T_{AN}. These trends may be a reflection of (a) short range order effects near T_{AN}: as mentioned earlier (chapter 1) smectic A like short range order develops in the N phase leading to better antiparallel molecular associations and more effective cancellation of longitudinal components of the dipole moments, and (b) the strong variation of local field with temperature which depends on the relative number of associated molecules and single molecules. In the case of 10 PMNBB (fig.4.10), $\varepsilon_\parallel$ exhibits a clear negative jump while $\varepsilon_\perp$ shows a less prominent increase as the sample is cooled across T_{AN}. The rates of decrease of $\varepsilon_\parallel$ and increase of $\varepsilon_\perp$ as the temperature is lowered in the A phase are somewhat

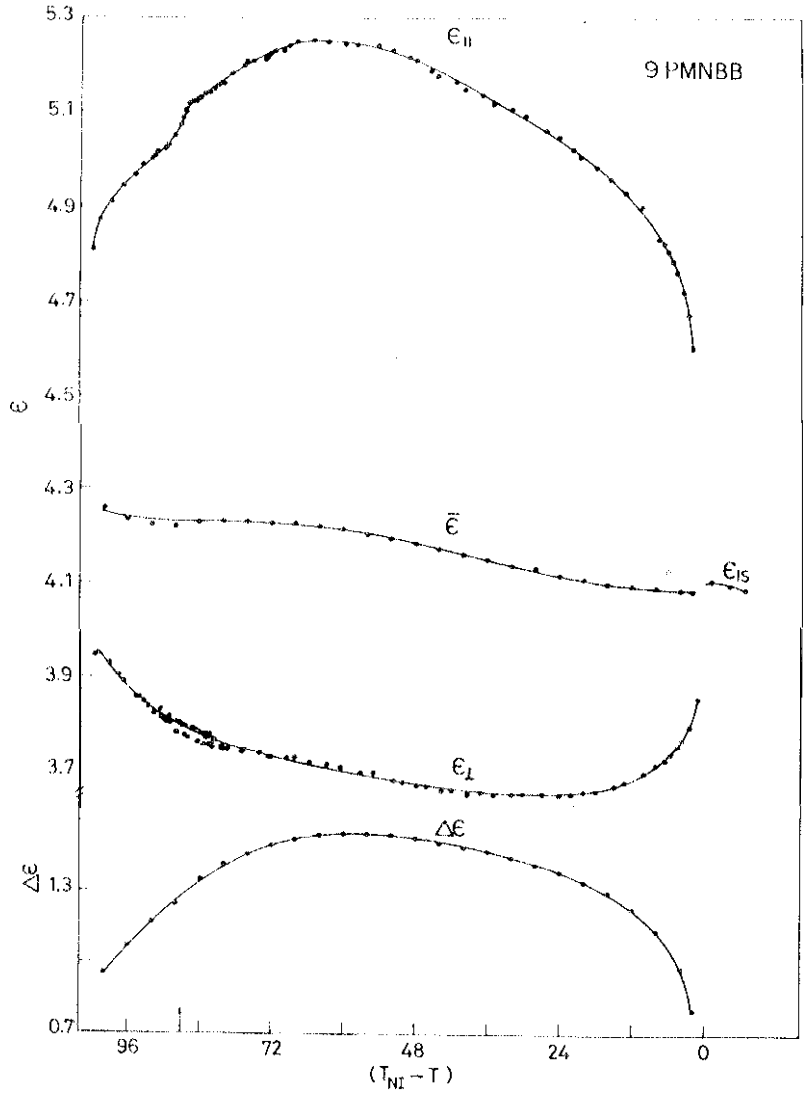

FIG.4.9: Temperature variations of the low frequency dielectric constants (upper section) and anisotropy (lower section? of 9 PMNBB measured at 1592 Hz. The arrow mark indicates T_{AN}.

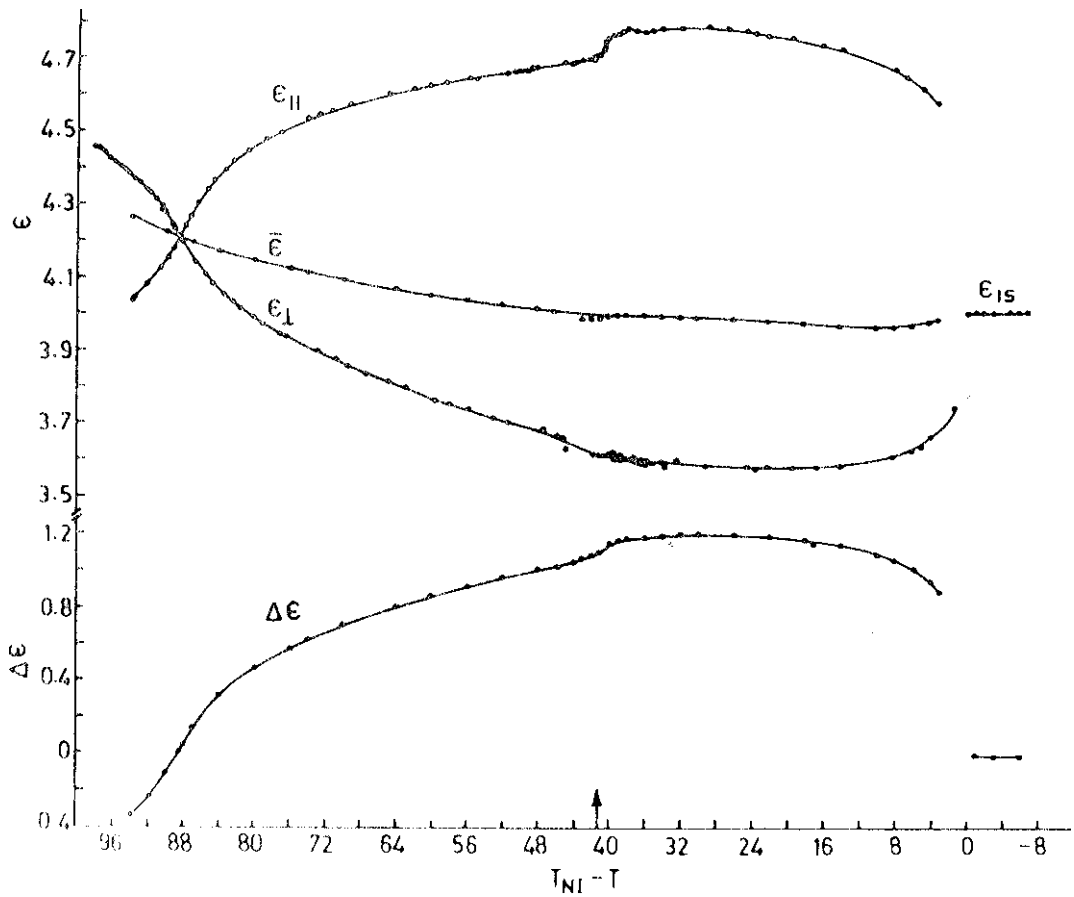

FIG.4.10: Temperature variations of the low frequency dielectric constants (upper part) and anisotropy (lower part) of 10 PMNBB measured at 1592 Hz. The arrow mark indicates T_{AN}.

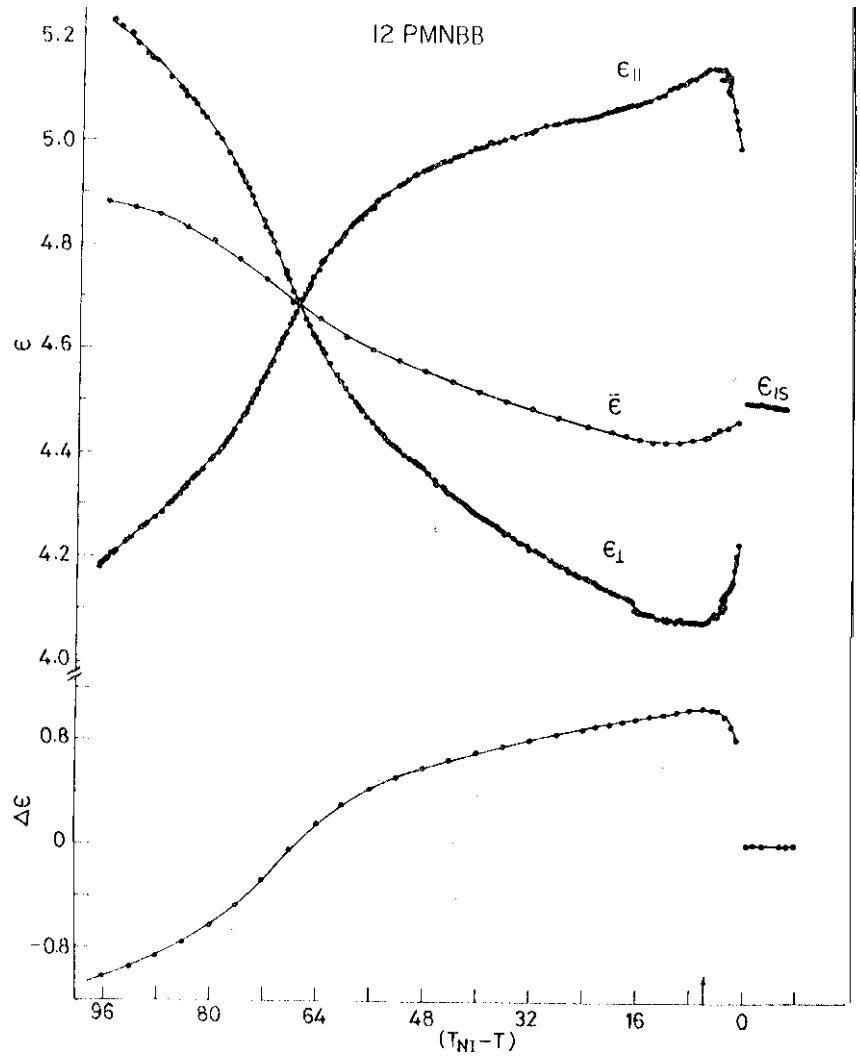

FIGURE 4.11

Temperature variations of the low frequency dielectric constants (upper part) and anisotropy (lower part) of 12 PMNBB measured at 1592 Hz. The arrow mark indicates T_{AN}.

similar. $\Delta\varepsilon$ decreases continuously in the A phase and changes sign becoming negative at $T_{NA} - T \simeq 90°C$. $\bar{\varepsilon}$ shows a general increase with decrease of temperature while actually $\bar{\varepsilon}$ decreased with decrease of temperature in the cyano compound (12 PMCBB, fig.4.4). This result most probably means that the cancellation of the longitudinal components of the NO_2 dipole moments of hue, associated molecules (fig.4.6c) is, not as effective as in the case of cyano compounds because the interactions between the lateral components of the dipole moments of the NO bonds would be repulsive on the average and would contribute to a reduction in the attractive interactions between the end groups. The influence of $\varepsilon_\perp$ with decrease of temperature has already been discussed and its influence predominates in the temperature variation of $\bar{\varepsilon}$.

In the case of 12 PMNBB (fig.4.11), $\varepsilon_\parallel$ increases and $\varepsilon_\perp$ decreases with decrease of temperature in the N phase and then $\varepsilon_\parallel$ decreases and $\varepsilon_\perp$ increases as the temperature is lowered in the A phase. The absence of pretransitional effects above T_{AN} is due to the relatively strong first order transition in this compound. The rates of variations become somewhat stronger at $T_{NI} - T \simeq 70°C$ at which temperature $\Delta\varepsilon$ itself changes sign. At still lower temperatures, the rates of variation level off.

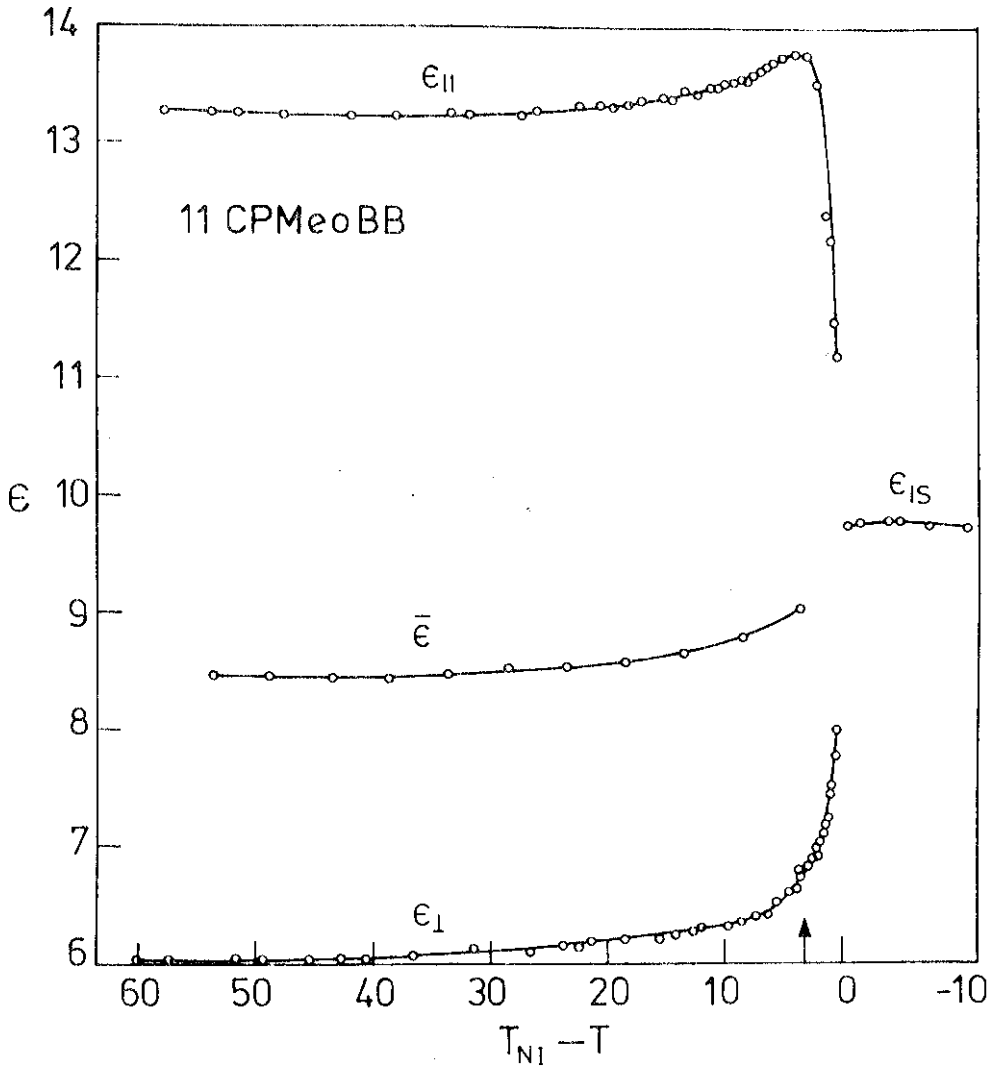

FIGURE 41 2

Temperature variations of the low frequency dielectric constants of 11 CPMeOBB measured at 1592 Hz. The arrow mark indicates T_{AN}.

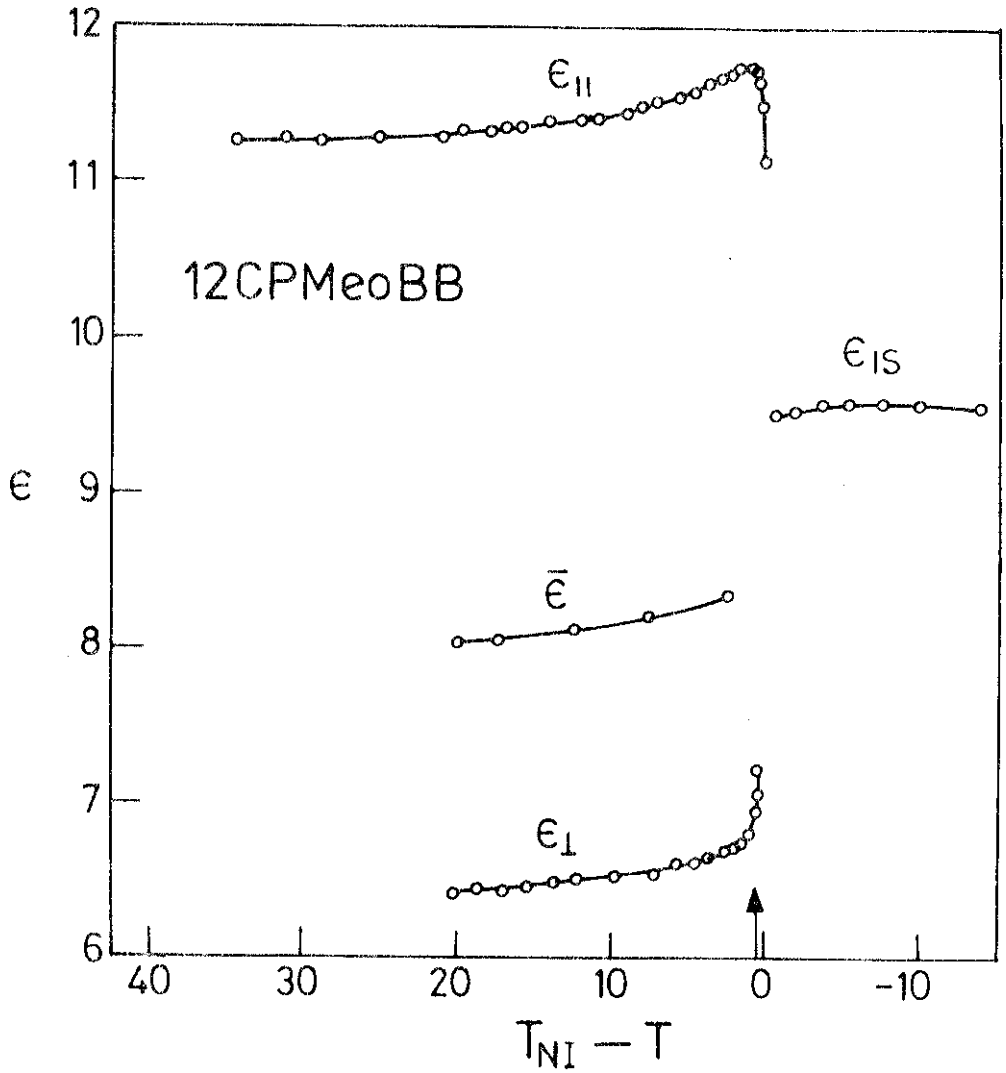

FIGURE 4.13

Temperature variations of the low frequency dielectric constants of 12 CPMeOBB measured at 1592 Hz. The arrow mark indicates T_{AN}.

is again due to the reduction of number of antiparallel pairs as the temperature is increased in the isotropic phase. $\varepsilon_{\parallel}$ decreases as the temperature is lowered in the A phase. As we have already discussed, pair formation is more effective at lower temperatures, and this leads to an effective lowering of the dipole moment along the long axis at the molecules and hence bo the observed reduction in $\varepsilon_{\parallel}$.

The dielectric constants of 11 PMeOBrBB are shown in fig.4.14. The compound exhibits a negative dielectric anisotropy, $\simeq -0.5$ at $T_{NI} - T \simeq 20°C$. $\bar{\varepsilon}$ decreasing with increase of temperature as is to be expected in the absence of any associations between strongly polar groups.

As we have indicated, the results of dielectric studies can be understood in terms of the model of associated pairs breaking up with increase of temperature. It is interesting to note that the decrease of $\Delta\varepsilon$ with lowering of temperature in the smectic phase in all the compounds which exhibit large bilayer spacings, is somewhat similar in shape to the increase of the layer spacing in the corresponding cases (chapter III), i.e., $(\varepsilon_{\parallel} - \varepsilon_{\perp})$ varies approximately like $\underline{d}$, as can be expected from our earlier discussion.

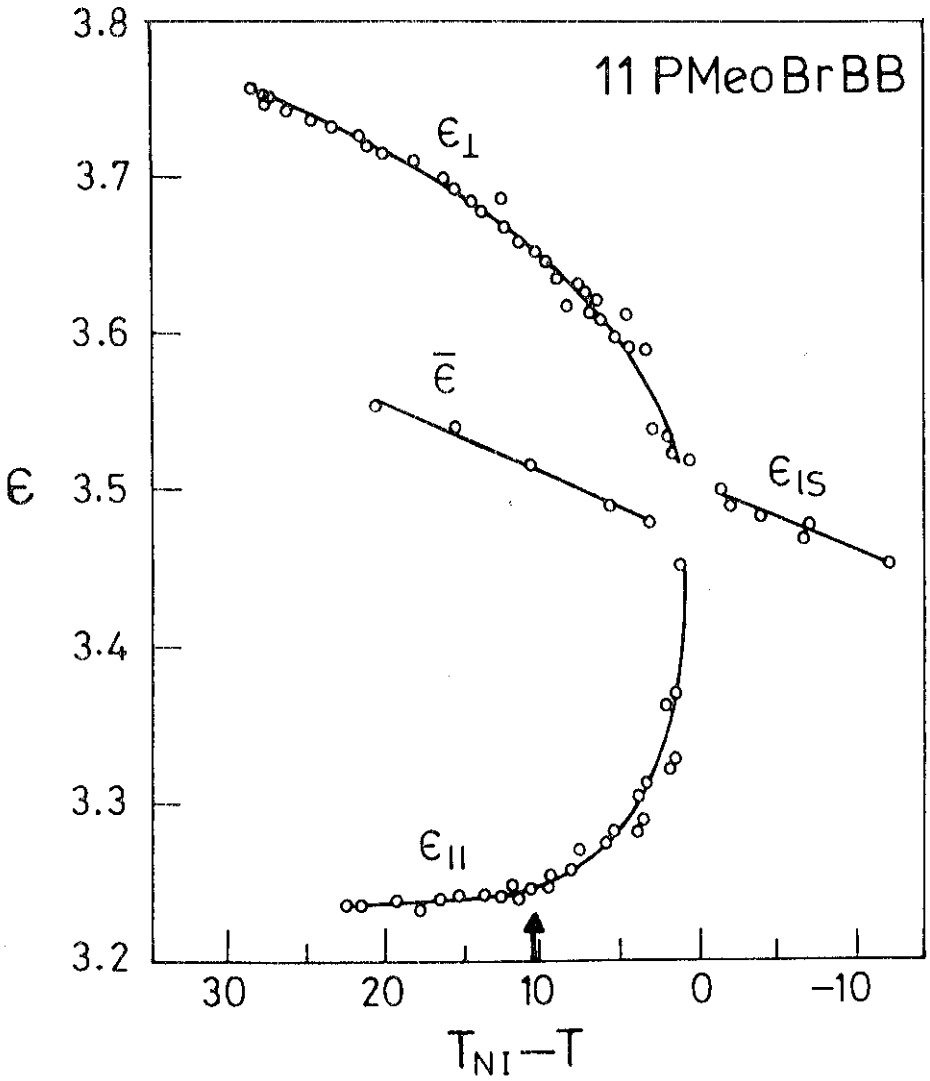

FIGURE 4.14

Temperature variations of the Low frequency dielectric constants of 11 PMeOBrBB measured at 1592 Hz. The arrow mark indicates T_{AN}.

(ii) Dielectric relaxation

The dielectric dispersion was measured up to 13 MHz. In fig.4.15, we have plotted the dielectric loss ($\varepsilon''_{\parallel}$) as a function of frequency for 11 CPMeOBB at different temperatures. $\varepsilon''_{\parallel}$ relaxes at a frequency of $\simeq$90 KHz at the lowest temperature of measurement in the A phase ($\sim$80°C), the frequency shifting to higher values at higher temperatures. The relaxation frequencies at various temperatures are also given in table 4.2. One of the curious trends noted for the compound is that the peak of $\varepsilon''_{\parallel}$ has practically the same level at all temperatures. One would normally expect a progressive reduction in this level as the temperature is increased since the orientation polarization which determines the height of this peak is reduced at higher temperatures due to the decrease of the orientational order parameter. As was discussed in chapter III, the attractive interactions between the neighbouring 11 CPMeOBB molecules are very weak due to the presence of the bulky lateral methoxy substituent and hence the bilayer structure with an overlap of the aromatic cores (as in fig.4.6a) is also fragile and the molecules tend to breakaway from such a structure at higher temperatures. This means that the effective dipole moment per molecule increases with

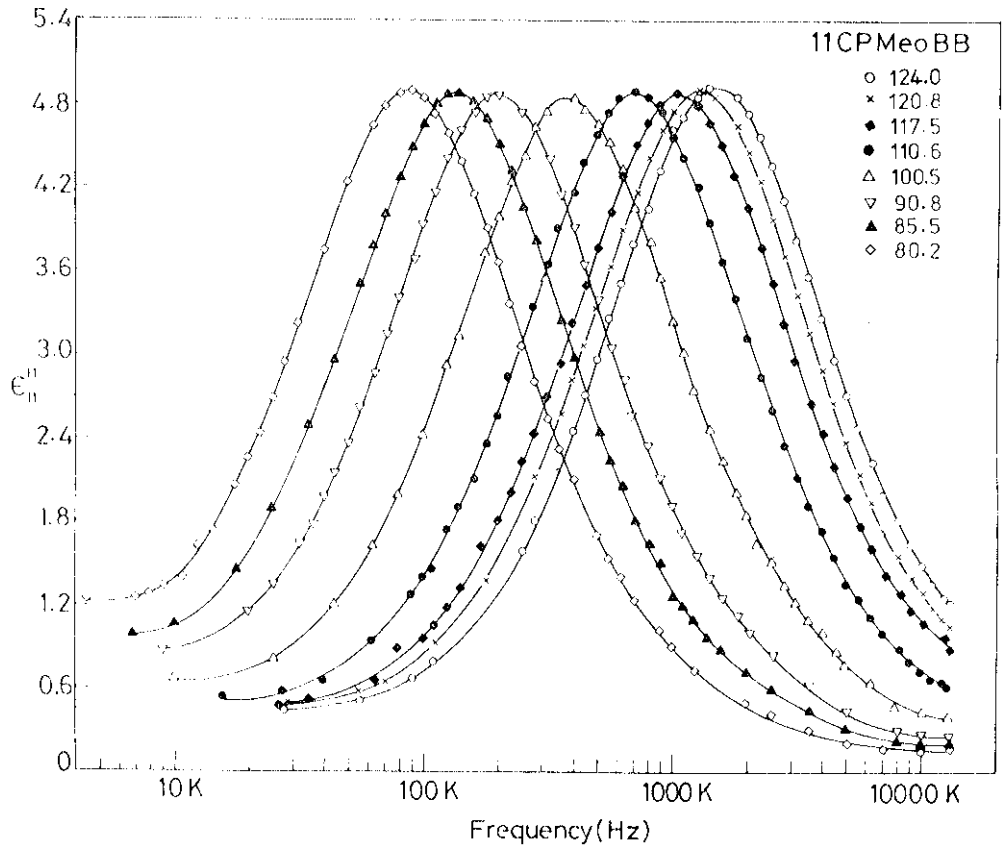

FIGURE 4.15

Frequency dependence of ϵ''_{11} (dielectric loss) at various temperatures in the smectic A phase of 11 CPMeOBB. The numbers against the symbols indicate the temperatures in ^{o}C.

Table 4.2

Relaxation frequencies

Temperature (°C)	Relaxation frequency(KHz)	Temperature (°C)	Relaxation frequency(KHz)
11 PMeOCBB		**11 CPMeOBB**	
130.6	2000	124.0	1500
		120.8	1250
128.5	1500	117.5	1050
		110.6	710
126.8	1250	100.5	390
124.5	1150	90.8	200
		85.5	140
114.0	580	80.2	90
108.0	400	**12 CPMeOBB**	
101.0	260	127.5	2100
		125.3	1750
94.5	175	120.5	1400
		114.8	1000
87.4	105	110.0	800
80.4	62	103.3	540

increasing temperature and thus the orientational polarization does not have the normal decreasing trend. Indeed the Cole-Cole plot which is a semicircle (fig.4.16) is practically identical at all temperatures in the A phase. The same trend is observed fn 12 CPMeOBB also (figs.4.17 and 4.18). The $\epsilon''_{\parallel}$ peak in this cure is 3.8 compared to 4.9 of 11 CPMeOBB as the effective dipole moment per unit volume is lower for the higher homologue. As in the Xray studies (chapter III), the effect of the breaking up of the bilayer structure (now as in fig.4.6c) is even more spectacular in the case of 11 PMeOCBB. The $\epsilon''_{\parallel}$ peak actually increases with increase of temperature from $\sim$1.16 at 80°C to $\sim$1.36 at 114°C in the A phase *(fig.* 4.1. On the other hand, la the B phase, there is a slight reduction in the peak value of $\epsilon''_{\parallel}$ with increase of temperature (fig.4.20). As we have discussed earlier in chapter III, the bilayer structure tn this case is very fragile and thus the number of free molecules is larger with a corresponding enhancement of the effective dipole moment at higher temperatures. As is to be expected, the $\epsilon''_{\parallel}$ peak *is* much smaller than in 11 CPMeOBB since the effective long axis component of the permanent dipole moment 14 much smaller in the case of 11 PMeOCBB (see fig.4.6). The Cole-Cole plot (fig.4.21) also brings

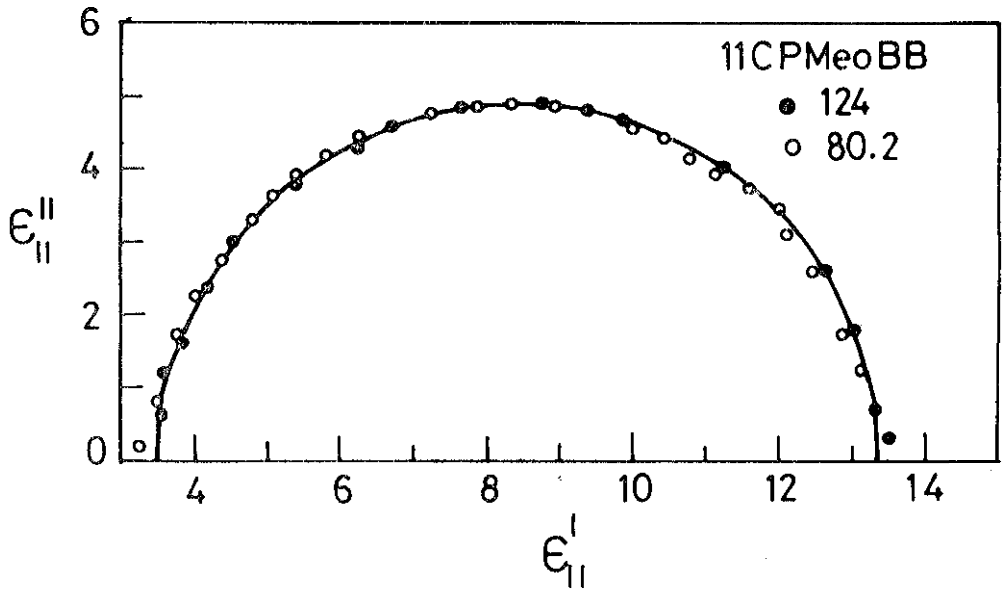

FIGURE 4.1 6

Cole-Cole plot for ϵ_{11} relaxation in the case of 11 CPMeOBB. The numbers against the symbols indicate the temperatures in ^{o}C.

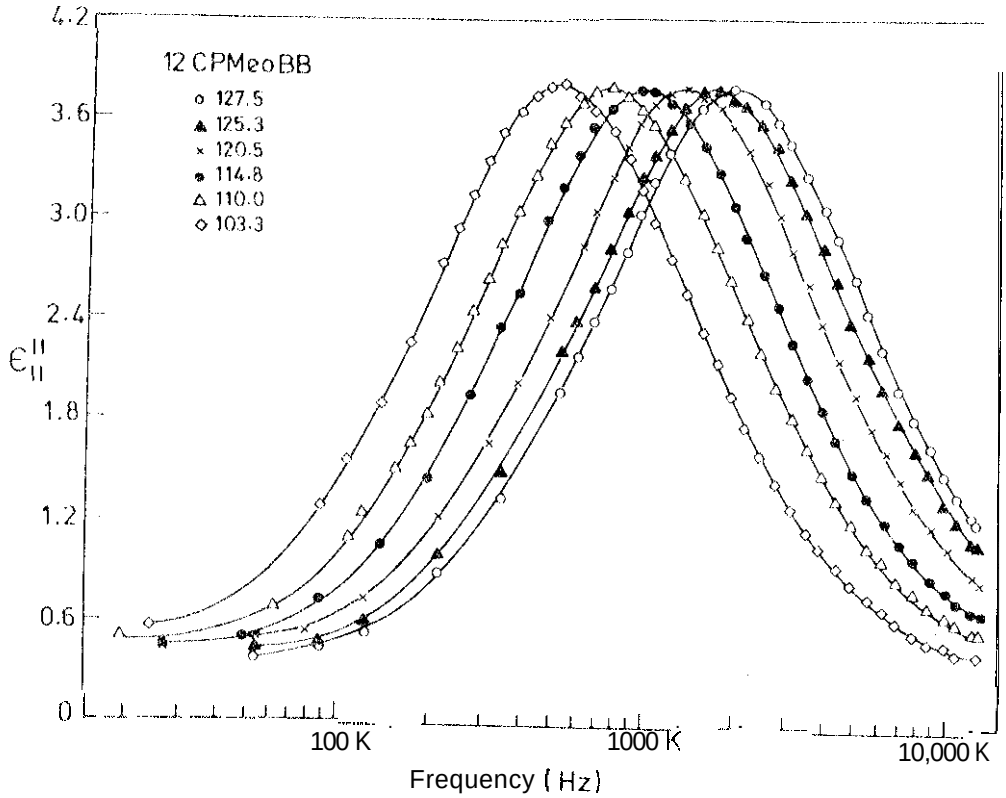

FIGURE 4.17

Frequency dependence of $\epsilon''_{\parallel}$ at various temperatures (indicated against the different symbols) in the smectic A phase of 12 CPMeOBB.

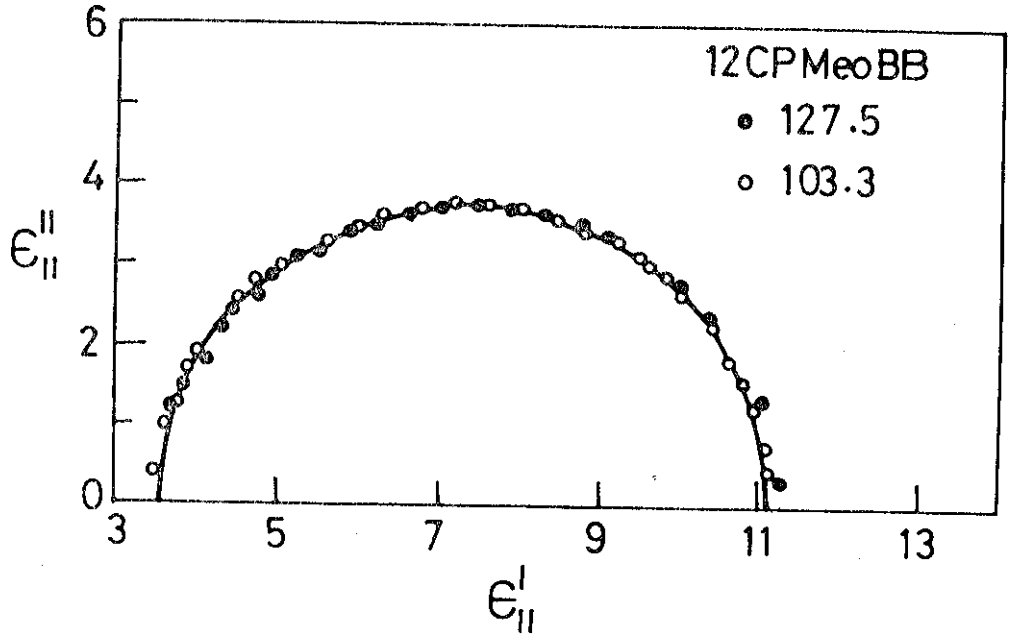

FIGURE 4.18

Cole-Cole plots lor $\epsilon_{\parallel}$ relaxation in the case of 12 CPMeOBB at two different temperatures (^{o}C).

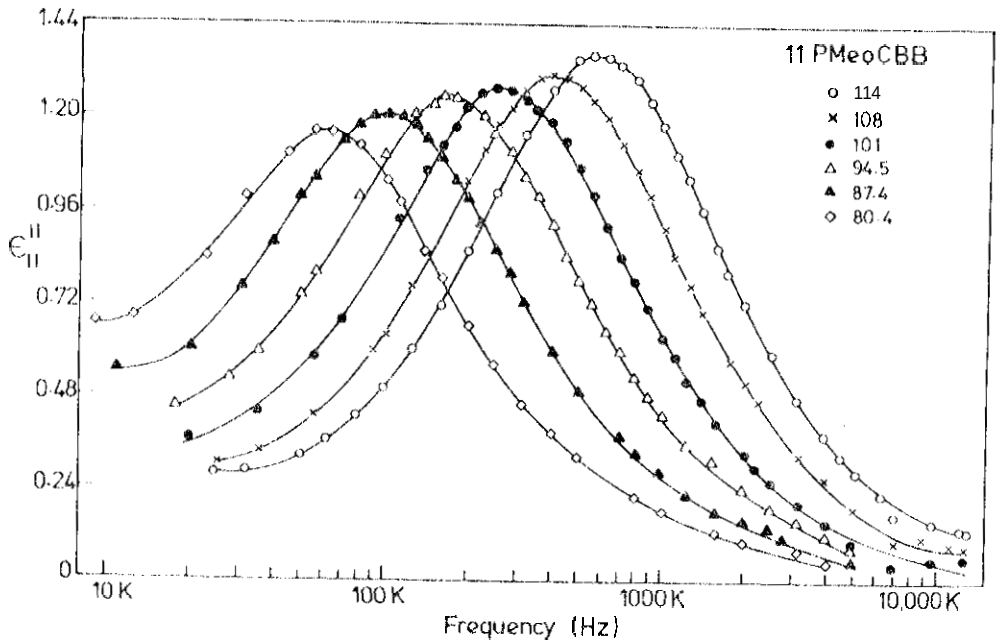

FIGURE 4.19

Frequency dependence of $\epsilon''_{\parallel}$ at various temperatures (shown against different symbols) in the smectic A phase of 11 PMeOCBB.

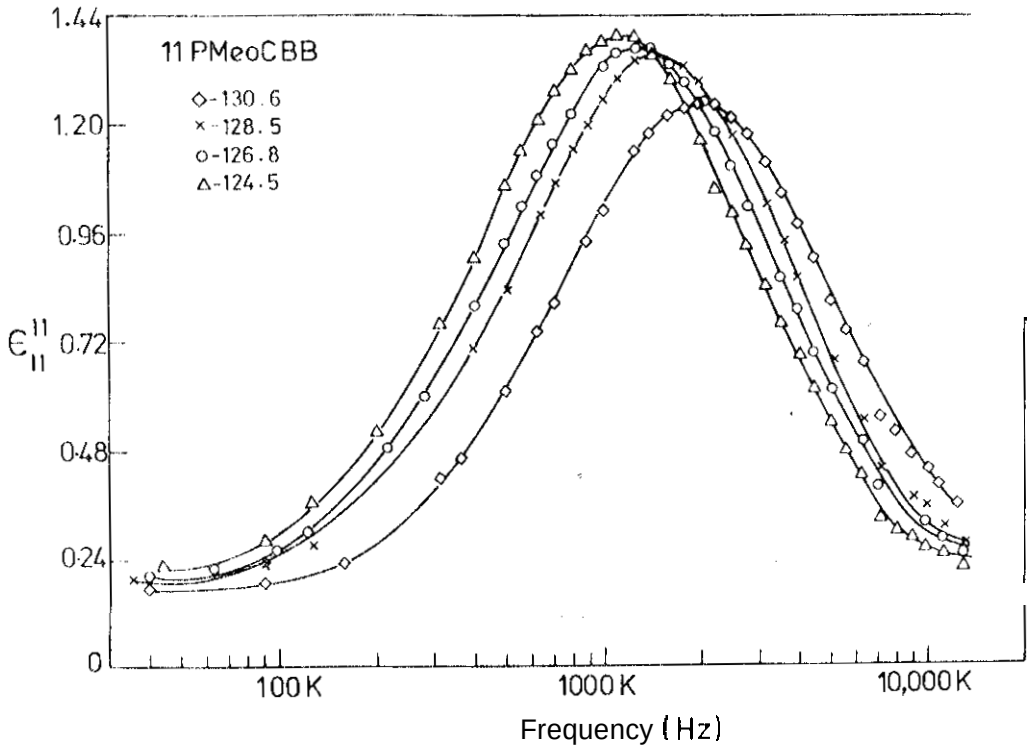

FIGURE 4.2B

Frequency dependence of ϵ_{11}^{11} at various temperatures (indicated against different symbols) in the nematic phase (N) of 11 PMeOCBB.

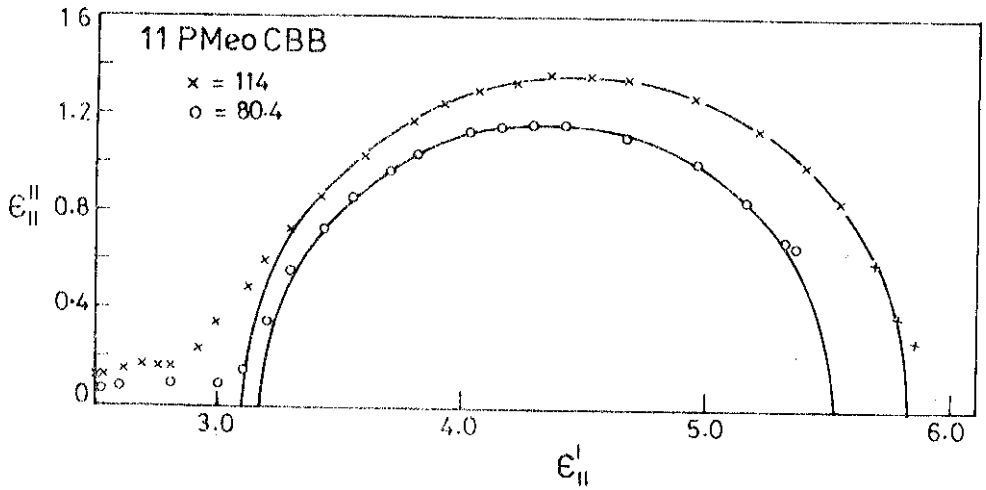

FIGURE 4.21

Cole-Cole plot for $\epsilon_{\parallel}$ relaxation in the case of 11 PMeOCBB at two different temperatures (°C).

out the fact that there are additional relaxations at higher frequencies for this compound, unlike in the case of 11 OPMeOBB. This is probably caused by the relaxation of the reorientational motion of μ_t, the component of the dipole moment perpendicular to the long axis. The equation for the overall dipole moment along the director which arises due to the imperfect order in the medium (represented schematically la fig.4.22) is given by[29]

$$\langle \mu_{\parallel}^2 \rangle = \frac{1}{3}\mu_L^2(1 + 2S) + \frac{1}{3}\mu_t^2(1 - S) \qquad (4.6)$$

where μ_L and μ_t axe the dipole moments along and perpendicular to the molecule and S ($=\langle(3\cos^2\theta - 1)/2\rangle$) is tho orientational order parameter. A similar equation can be written for the overall dipole moment perpendicular to the director

$$\langle \mu_{\perp}^2 \rangle = \frac{1}{3}\mu_L^2(1 - S) + \frac{1}{3}\mu_t^2(1 + \frac{S}{2}) \qquad (4.7)$$

The influence of μ_L is not usually seen in tho $\varepsilon_\perp$ relaxation, since the reorientational motion of μ_L is a much slower process than both the librational motion (about the director) of the molecules and hha reorientation of μ_t about the long axis. $\varepsilon_\perp$ of 11 PMeOOBB shows a very broad relaxation (fig.4.23 and 4.21)) with a brood maximum $\sim$6 MHz. This appears to be a particularly low frequency for the

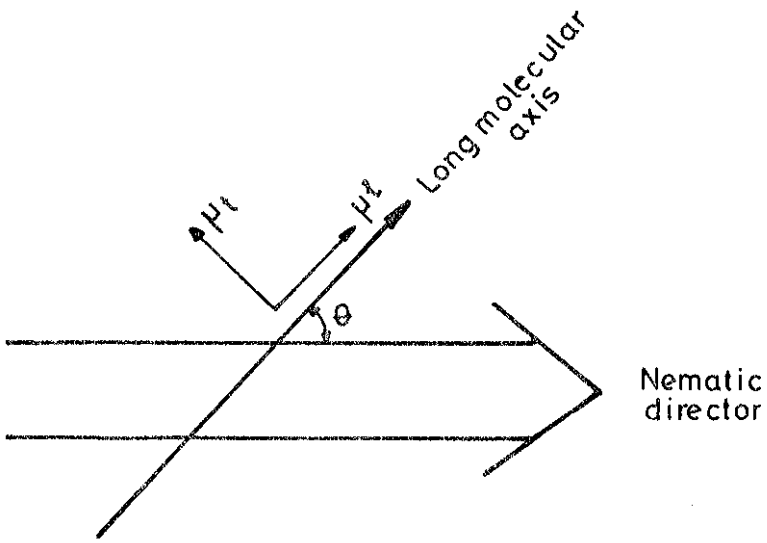

FIGURE 4.22

Schematic representation of dipole components in an aligned nematic. (Reproduced from ref. 29).

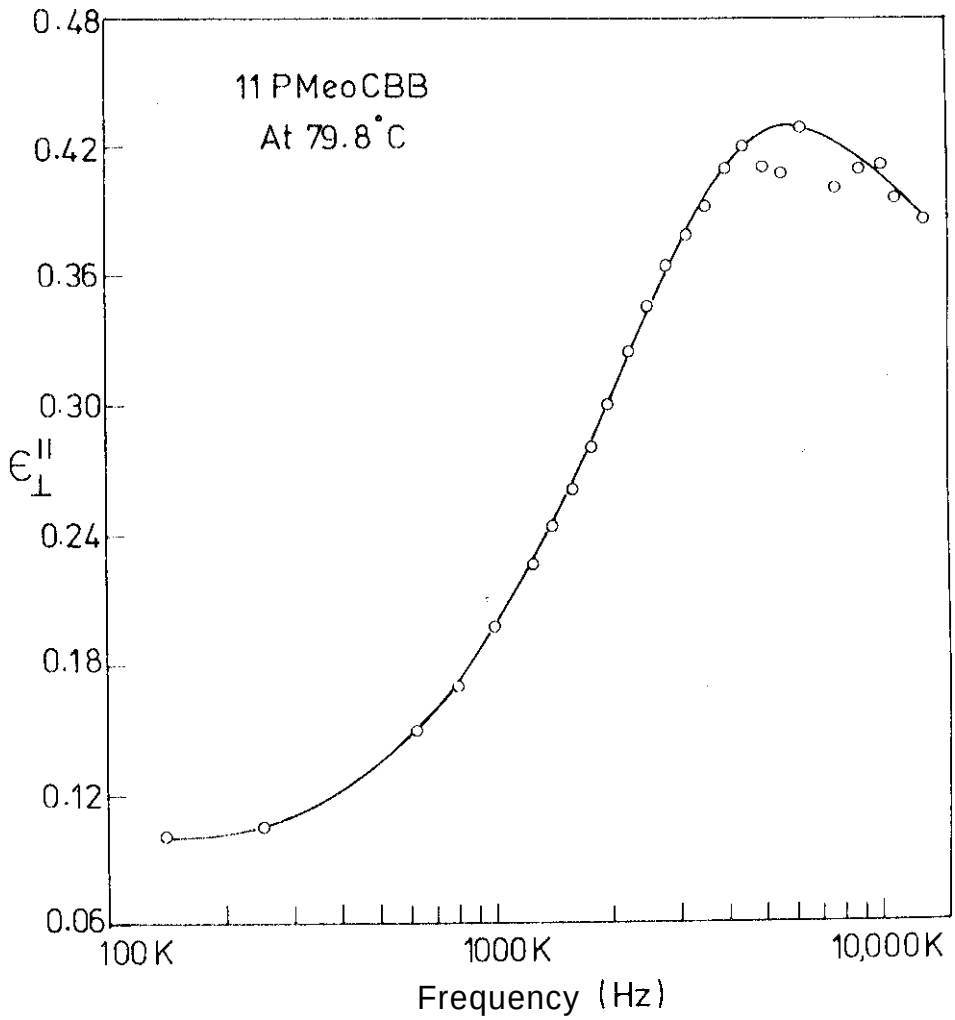

FIGURE 4.23

Frequency dependence of $\epsilon_{\perp}^{II}$ in the case of 11 PMeOCBB.

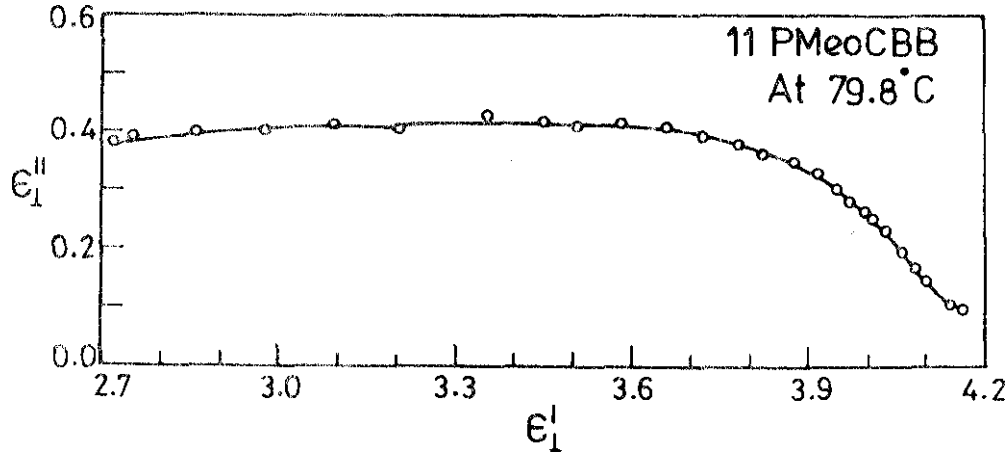

FIGURE 4.24

Cole-Cole plot for $\epsilon_\perp$ relaxation in the case of 11 PMeOCBB.

relaxation of $\mu_\perp$ and in contrast we did not see any indication of $\epsilon_\perp$ relaxation in 11 CPMeOBB in this frequency range. Obviously the structure characterised by the large bilayer spacing is responsible for this relaxation. If the molecular pairs which have an overlapping region only near the cyano end groups reorient as a single unit, we could expect a lowering of the relaxation frequency, for the moment of inertia of the pals reorienting about an axis which is tangential to the surface of contact of the two molecules is much larger than that for a single molecule reorienting about its long axis. Further, the pair would have much greater probability of colliding against neighbouring pairs or individual molecules in the reorientation process and hence the effective friction coefficient would also be large. Thus the relaxation occurs at a fairly low frequency. Indeed measurements at higher frequencies can be expected to show another relaxation of due to the reorientation of the individual molecules about their long axes. The $\mu_\parallel$ relaxation of pairs is also reflected in the dispersion of $\epsilon_\parallel$, as we saw in fig.4.21. The Cole-Cole plot corresponding to $\epsilon_\perp$ (fig.4.24) also shows that the dispersion is characterised by a rather broad distribution of relaxation times. A 'broad distribution is indeed expected for the $\epsilon_\perp$ relaxation as the

libration of the molecules about the short axis contributes to this relaxation process. The molecular order and hence the local field is not well defined in this direction. The barrier height for reorientation is so small that only a distribution of relaxation times can be expected.[19] Further, in the case of I1 PMeOCBB there are more than one species (pairs which overlap at the end groups only, those with overlap of the entire aromatic core and individual molecules) which could also contribute to the extremely broad distribution of relaxation times seen in fig.4.24.

We shall now return to a further discussion on the dispersion of $\varepsilon_{\parallel}$. It is interesting to note that I1 PMeOCBB and I1 CPMeOBB tend to have the same value of $\varepsilon_{\parallel}$ at frequencies just greater to that of relaxation, the value being $\simeq 3$ at the lowest temperature of measurement. This is understandable, since at these frequencies the contributions to $\varepsilon_{\parallel}$ arise from the induced dipole moment along the long axes of the molecules and induced as well as permanent dipoles perpendicular to the long axes (eqns. 4.6 and 4.7).[29] These contributions are practically the same in the two compounds. However, in the case of I1 PMeOCBB as the frequency is further raised to $\sim$13 MHz $\varepsilon'_{\parallel}$ begins to decrease again

since the orientational polarization perpendicular to the long; axes relaxes as we discussed earlier.

By plotting ln f_R against 1/T where f_R is the relaxation frequency corresponding to the maximum in ε'' and T the absolute temperature, we get straight line graphs in the N and A phases as shown in fig.4.25 *fox* 11 PMeOCBB, and in the A phase of 11 OPMeOBB and 12 OPMeOBB (figs. 4.26 and 4.27 respectively). The measurements could not be made in the N phase of the latter two compounds because of the very short range of existence of that phase in both the cases (table 4.1). The slopes of We lines give the activation energies which are listed in table 4.3 for all the three compounds studied. It is interesting to note that the activation energy is practically the same in the A phases of both 11 OPMeOBB and 11 PMeOCBB. The activation energy is lower in the A phase than in the N phase of 11 PMeOCBB. The latter result has been found earlier la several studies on compounds exhibiting both N and A phases.[30-32] The activation energy is a sum of both the rotational potential barrier against flipping about the short axis and dissipation due to the friction coefficient which is effective against such a rotational diffusion. Hence the lowering of the activation energy

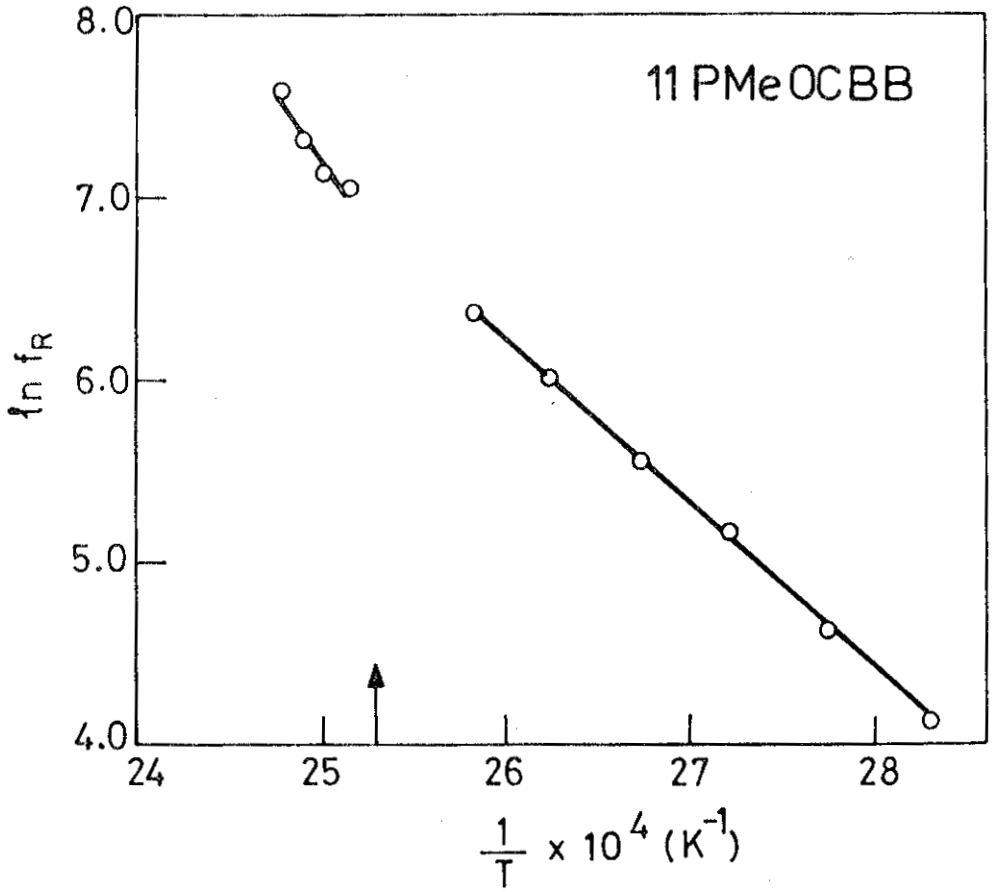

FIGURE 4.25

Plot of ln f_R against 1/T in the smectic A and nematic phases of 11 PMeOCBB, where f_R is the relaxation frequency. The arrow mark indicates T_{AN}.

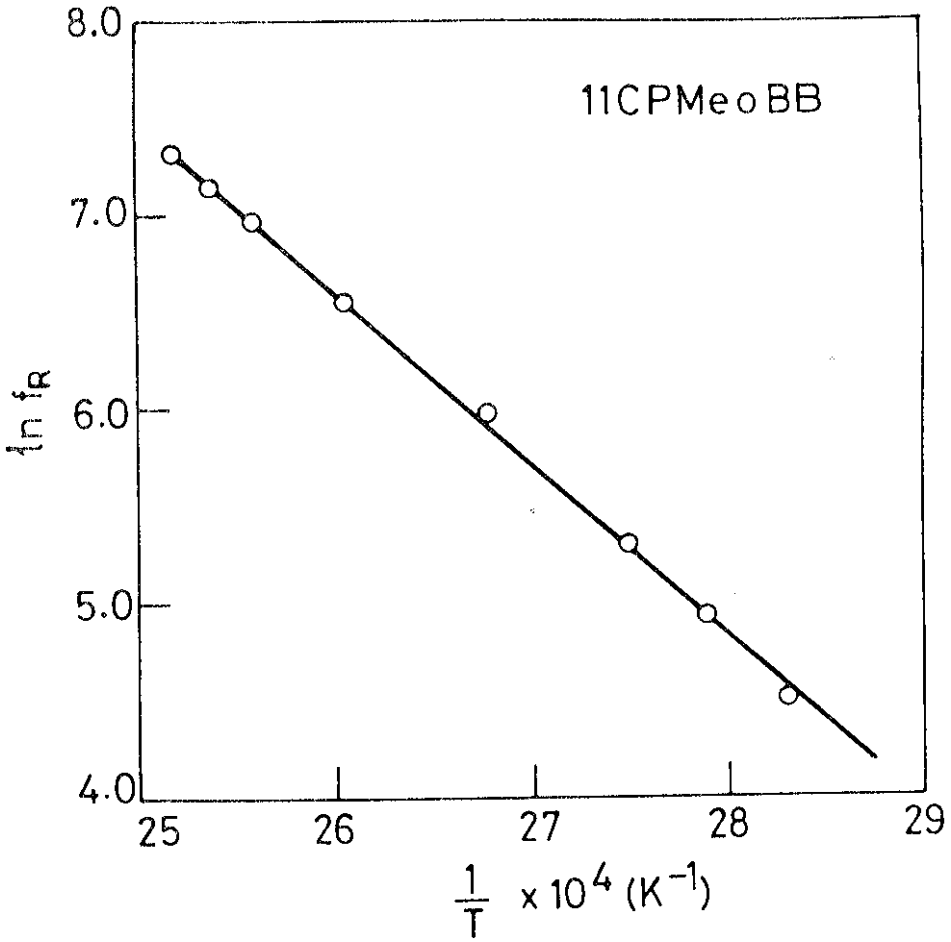

FIGURE 4.26

Plat of ln f_R against 1/T in the smectic A phase of 11 CPMeOBB, whore f_R is the relaxation frequency.

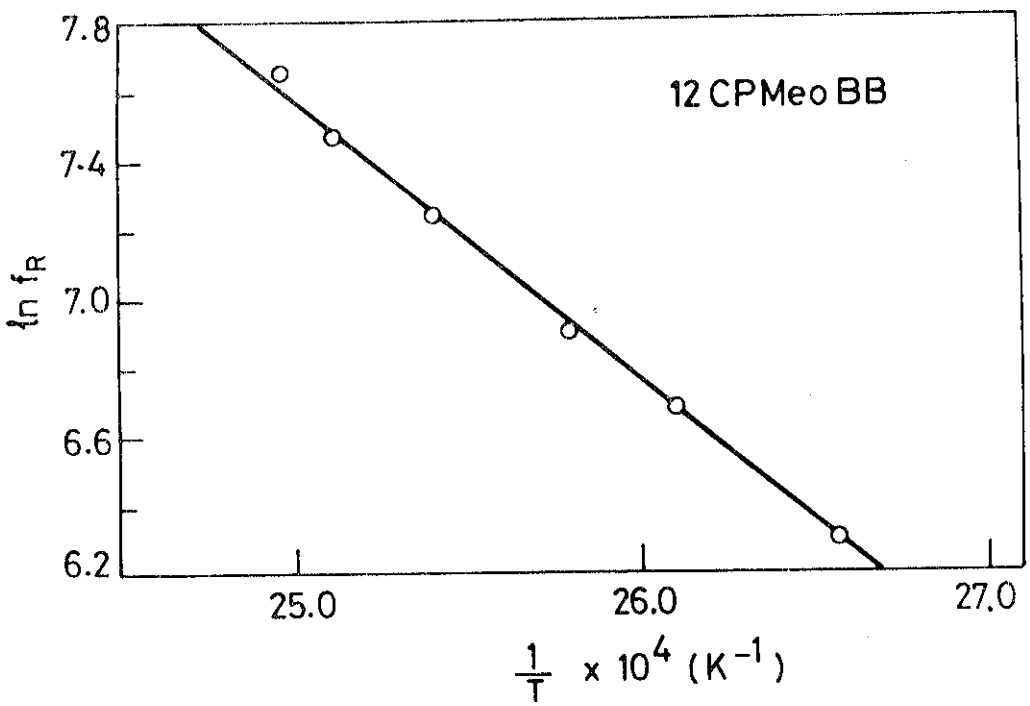

FIGURE 4.27

Plot of in f_R against 1/T in the smectic A phase of 12 CPMeOBB, where f_R is the relaxation frequency.

Table 4.3

Activation energies in eV in the smectic A and nematic phases

Compound	Smectic A	Nematic
11 OPMeOBB	0.75	-
12 OPMeOBB	0.7	-
11 PMeOOBB	0.78	1.27

in the A phase is somewhat puzzling or one would expect that at least the orientational potential barrier would be higher due to the higher order parameter in fhe A phase. Druon and Wacrenier[33] have argued that in the care of bilayer smectics that the two neighbouring molecules have an asymmetric potential energy curve as a function of the angle between their long axes (fig.4.28). They assumed that in the N phase the asymmetry would disappear (i.e., $W_{SN} = W'_{SN}$). In the A phase the layering is supposed to bring in the asymmetry such that $W_{SA} > W'_{SA}$ and $W'_{SA} < W_{SN}$. If W_{SA} is very much greater than W'_{SA}, one can expect that the external field will not be able to disturb the molecular pairs in the antiparallel configuration (i.e., with energy W_{SA})[34] and only the molecules in the parallel configuration (with potential barrier W'_{SA}) would participate in the reorientation. As it is assumed that $W'_{SA} < W_{SN}$, the activation energy is lowered in the A phase. However, we must point out that it is unlikely that the anisotropy of the potential energy will vanish in the N phase. Druon and Wacrenier's argument still holds if the anisotropies in the two phases are such that $W'_{SA} < W'_{SN}$. In other words, the layering of the A phase helps to increase the repulsive interactions between cyano end groups of parallel molecules.

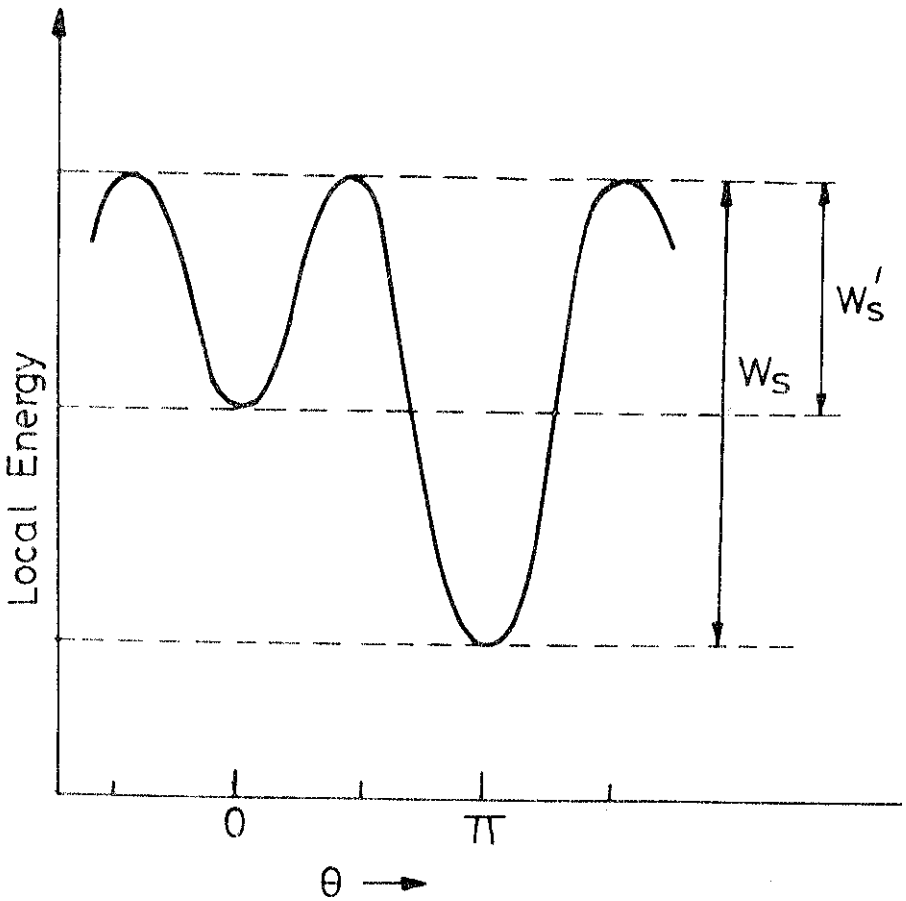

FIGURE 4.28

Schematic diagram depicting the variation of local energy of a pair of highly polar molecules as a function of the angle between their long axes (Reproduced from ref. 33).

Further, the lowering of activation energy is found not only in bilayer smectic A phases but also in monolayer smectics[35] in which the potential energy anisotropy is likely 40 bar quite small. Hence the origin of the phenomenon is to be sought in the layered arrangement of the A phase itself. In the following paragraphs, we will try to argue that two different mechanisms may be responsible for this effect.

Recently Edwards and Madden[36] have proposed a molecular theory of the dielectric permittivity of nematic liquid crystals in which intermolecular dipole-dipole correlations are explicitly taken into account. Following a procedure developed earlier by Sullivan and Deutch[37] for isotropic liquids, they have given the frequency dependence of the parallel and perpendicular components of the complex dielectric constant in terms of the dipole correlations which are of short range and under certain symplifying approximations have derived explicit expressions for the dielectric constants. From these expressions one can write for the relaxation time parallel to the director

$$\tau_{\parallel} = \tau_D \varepsilon_{\parallel} \left(\frac{\varepsilon_{\parallel} - 1}{\varepsilon - 1}\right) \qquad (4.8)$$

with a similar expression for $\tau_{\perp}$. Here τ_D is the usual

Debye relaxation time, $g_{\parallel}$ the retardation factor caused by the nematic potential and introduced by Meier and Saupe[19] as discussed earlier, and $\varepsilon_{\parallel}$ the static dielectric constant parallel to the director and ε the mean dielectric constant. The terms in brackets are new in this theory and arise from the dipole correlations in the medium. We assume that relation (4.8) can be used in the A phase also. The layering of the A phase gives rise to increased anti-parallel dipole correlations between the Zong axis components of dipoles. This has been found experimentally for several cases, including relatively weakly polar compounds.[27,38,39] Indeed such correlations lead So a lowering of $\varepsilon_{\parallel}$ as the temperature is decreased in the A phase as we can see from figs.4.4 and 4.7-4.13. On the other hand, in all these cases, $\varepsilon_{\perp}$ increases in the N phase with the lowering of temperature from T_{NI}. From relation (4.8) this means that effectively the relaxation time increases more rapidly with decrease of temperature in the N phase than that given by the retardation factor $g_{\parallel}$ alone. The opposite temperature variation of $\varepsilon_{\parallel}$ in the A phase leads to low $\tau_{\parallel}$ values in the A phase than in the N phase even if $g_{\parallel}$ is characterized by the same potential barrier q in the two phases. Thus the layering order present in the

A phase gives rise to a lowering a4 $\tau_{\parallel}$ or equivalently a higher value of the frequency of relaxation. Further, as the temperature is lowered in tho A phase, the smectia order parameter increases and hence this effect also increases. This is obviously equivalent to a lowering of the activation energy as can be seen, for example, from fig 4.25. In summary, the effect of the $(\epsilon_{\parallel} - 1)$ term in equation (4.8) is to increase the activation energy in the N phase and lower it in the A phase, thus leading to a considerable difference in the activation energies *of!* the two phases.

We also believe that a second mechanism may operate in the A phase due to packing effects. As we discussed earlier in chapter III, the thermal expansion in the A phase appears to be considerably anisotropic. Usually the layer spacing does not vary much with temperature in monolayer smectics, in the absence of bulky lateral substituents fa the molecules. A liquid is known to have 'voids' or 'holes' in its structure. One can expect that the nematic phase has a spatially uniform distribution of the 'holes'. When the transition to the A phase takes place, the fluidity becomes confined tc the layers. Hence the holes can be expected to be trapped within the layers. Consequently the number of

collisions that a molecule suffers in the reorientational motion can be smaller in the A phase[40] or the relaxation time can be lower or effectively the activation energy can be lower than in Oh8 N phase at the same density. For instance, this effect may be important in 4-n-octyloxy-4-cyanobiphenyl (8 OCB) which exhibits a bilayer A phase with hardly any temperature dependence of the layer spacing.[41] 8 OCB also exhibits a lower activation energy in the A phase than in the N phase (chapter VI). The packing effect may also explain the earlier observation of two activation energies in 11 CPMBB and 12 CPMBB[32] (figs. 4.29 & 4.30). As we noted earlier in chapter III, these compounds have a contraction of the layer spacing in the lower temperature range of the A phase but an expansion at higher temperatures (see figs. 3.20 and 3.21). The activation energy in the two regions is distinctly different, being lower in the lower temperature range. The layer expansion in the higher temperature range would imply that the thermal expansion is more isotropic in this range and thus the packing effects would increase the activation energy compared to that in the lower temperature range even though it is still smaller than that of the N phase.

As we discussed earlier in chapter III, in the

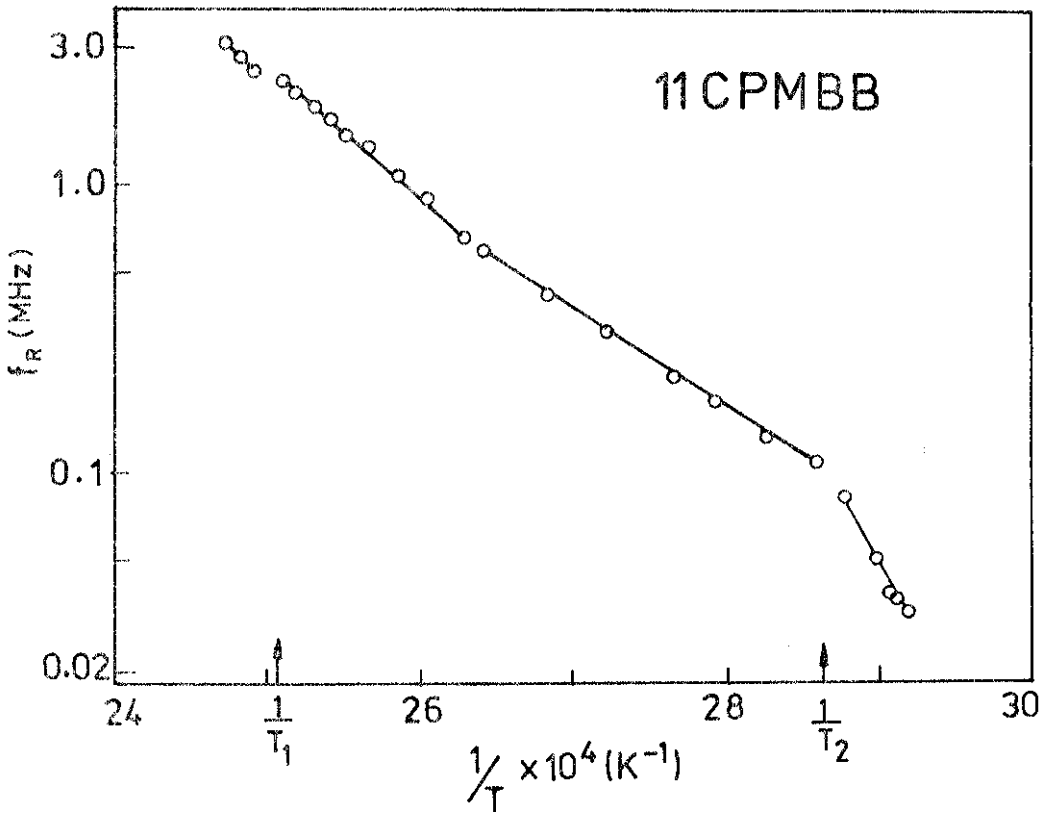

FIGURE 4.29

Plot of relaxation frequency (f_R) against 1/T for 11 CPMBB. T_1 is the normal nematic-smectic A transition temperature. T_2 is the smectic A - reentrant nematic transition temperature, (Reproduced from ref. 32).

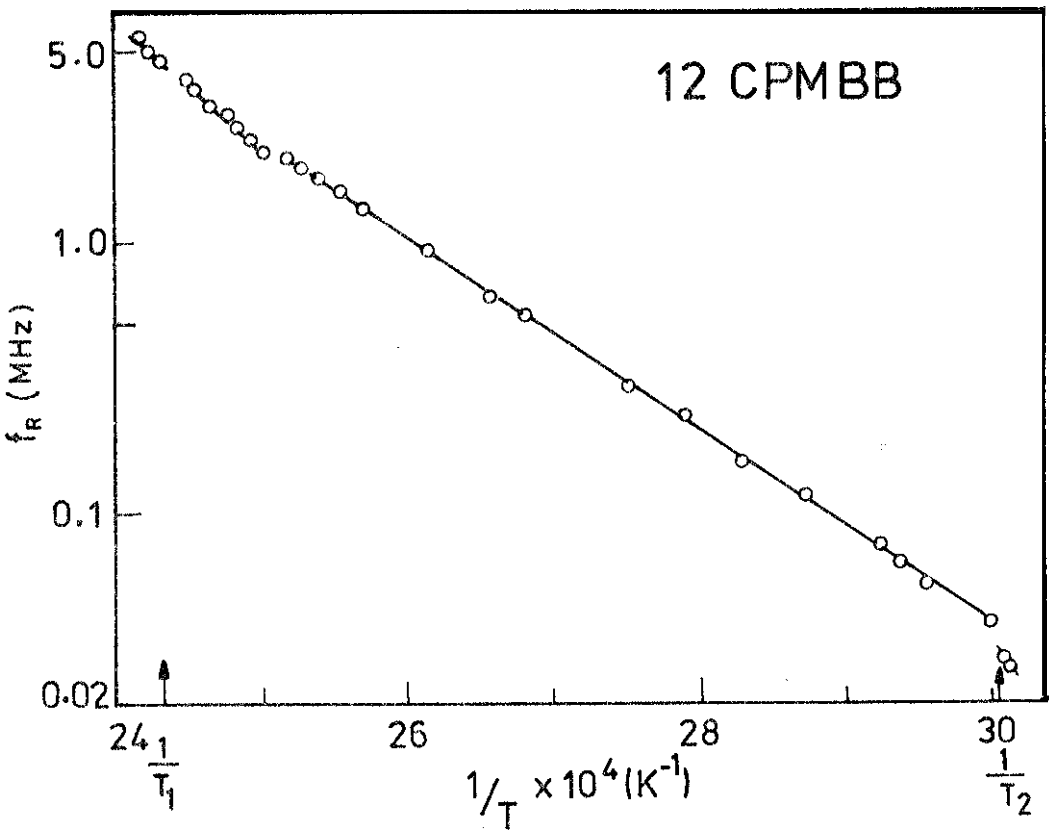

FIGURE 4.30

Plot of relaxation frequency (f_R) against 1/T for 12 CPMBB. T_1 is the normal nematfc - smectic A transition temperature, T_2 is the smectic A - reentrant nematic transition temperature. (Reproduced from ref. 32).

case of 11 PMeOBrBB the layer spacing increases considerably with temperature. But we could not study the influence sf this factor on the activation energies. The long axis component of the dipole moment la so low in 11 PMeOBrBB that no dispersion of $\epsilon_{\parallel}$ could be measured.

In conclusion, changes taking place in the bilayer structures of strongly polar compounds are found to have a profound influence on their dielectric properties. If the dipole moments of the linkage groups oppose that of the terminal polar group and the compounds have bulky lateral substituents, they possess bilayer structures with large bilayer spacings which are extremely sensitive to temperature and can exhibit reversal sf $\Delta\epsilon$ becoming negative at lower temperature. These changes in the bilayer structure are reflected in the relaxation process also. For instance, the peak value of $\epsilon''_{\parallel}$ in 11 PMeOCBB increases with increasing temperature though one would normally expect an opposite trend and $\epsilon_{\perp}$ shows a broad relaxation at $\sim$6 MHz which is a relatively low frequency for the relaxation in this direction. Further, the increased antiparallel correlation in the layered A phase compared to the N phase and the possible anisotropy in the expansion coefficient of the layered A phase appear

to give a lower activation energy for the low frequency dielectric relaxation of $\varepsilon_{\perp}$ in the A phase than in the N phase. Further investigations are necessary for a better understanding of the mechanism leading to the lowering of activation energy in the A phase than in Me N phase.

REFERENCES

1 W.Maier and G.Meier, Z.Naturforsch., 16a, 470 (1961); Z.Electrochem., 65, 556 (1961).

a W.H.de Jeu, Solid State Physics, Suppl. No.14, Ed. L.Liebert, Academic Press, New York (1978) p.109; see also W.H. de Jeu, Physical Properties of Liquid Crystalline Materials, Gordon & Breach, New York (1980).

3 M.Schadt, J.Chem.Phys. 56, 1494 (1972).

4 B.R.Ratna and R.Shashidhar, Pramana, 6, 278 (1976).

5 M.Schadt and W.Helfrich, Appl.Phys.Lett., 18, 127 (1971).

6 P.E.Cladis, Phys.Rev.Lett., 35, 48 (1975).

7 N.V.Madhusudana, B.K.Sadashiva and K.P.L.Moodithaya, Curr.Sci. 48, 613 (1979).

8 F.Hardouin, G.Sigaud, M.F.Achard and H.Gasparoux, Solid State Comm. 30, 265 (1979).

9 F.Hardouin, A.M.Levelut, G.Sigaud, Nguyen Huu Tinh and M.F.Achard, Invited talk presented at the Ninth Int.Liquid Cryst.Conf., Bangalore (1982).

10 A.J.Leadbetter, R.M.Richardson and C.N.Colling, J.de Phys. 36, C1-37 (1975).
Also see, A.J.Leadbetter, J.C.Frost, J.P.Gaughan, G.W.Gray and A.Mosley, J.de Phys. 40, 375 (1979); J.E.Lydon and C.J.Coakley, J. de Phys. 36, C1-45 (1975).

11 W. Maier and G.Meier, Z.Naturforsch., 16a, 262 ((1961); ibid., 16a, 470 (1961).

12 L.Onsager, J.Am.Chem.Soc., 58, 1486 (1936). Also see C.J.F.Bottcher, Theory of Electric Polarisation, Elsevier (1973).

13 W.Maier and A.Saupe, Z.Naturforsch., 13a, 564 (1958); ibid., 14a, 882 (1959); 15a, 287 (1960).

14 S.Chandrasekhar and B.R.Ratna, Mol.Cryst.Liq.Cryst. Lett., 82, 193 (1982).

15 W.H.de Jeu and Th.W.Lathouwers, Z.Naturforsch., 29a, 905 (1974).

16 B.R.Ratna and R.Shashidhar, Mol.Cryst.Liq.Cryst. 42, 113 (1977).

17 N.V.Madhusudana and S.Chandrasekhar, Proc. Int. Liq. Cryst. Conf., Bangalore, 1973, Pramana Suppl. 1, p.57.

18 W.Maier and G.Meier, Z.Naturforsch, 16a, law (1961).

19 G.Meier and A.Saupe, Mol. Cryst. 1, 515 (1966); A.J.Martin, G.Meier and A.Saupe, Symp.Faraday Soc. 5, 119 (1971).

20 P.Debye, 'Polar Molecules', Chemical Catalog Co.(1928).

21 K.S.Cole and R.H.Cole, J.Chem.Phys. 9, 341 (1941).

22 D.Lippens, J.P.Parneix and A.Chapoton, J.de Phys. 38, 1465 (1977).

23 M.Subramanya Raj Urs (to be published).

24 M.Subramanya Raj Urs and V.Surendranath, Mol.Cryst. Liq.Cryst. 99, 279 (1983).

B.R.Ratna and R.Shashidhar, Mol.Cryst.Liq.Cryst. 42, 185 (1977).

V.I.Minkin, O.A.Osipov and Y.A.Zhdanov, Dipole Moments in Organic Chemistry (Plenum Press, New York) 1970.

27 L.Benguigui, J. de Phys. 40, 705 (1979).

28 G.J.Sprokel, Mol.Cryst.Liq.Cryst. 42, 233 (1977).

29 A.Buka, P.G.Owen and A.H.Price, Mol.Cryst.Liq.Cryst. 51, 273 (1979).

30 C.Druon and J.M.Wacrenier, Ann. Phys. 3, 199 (1978).

31 L.Bata and A.Buka, Acta Physica Polonica, A54, 635 (1978).

B.R.Ratna, R.Shashidhar and K.V.Rao, Proc. Int. Liq.Cryst.Conf., Bangalore, 1979, Ed. S.Chandrasekhar (Heyden, London) 1980, p.135.

C.Druon and J.M.Wacrenier, Mol.Cryst.Liq.Cryst. 88, 99 (1982).

34 J.D.Hoffmann and H.G.Pfeiffer, J.Chem.Phys. 22, 132 (1954).

35 A.Buka and L.Bata, in Advances in Liquid Crystals, Vol. I, Ed. L.Bata (Pergamon, Oxford, 1980) p.261.

36 D.M.P.Edwards and P.A.Madden, Mol.Phys. 48, 471 (1983).

37 D.E.Sullivan and J.M.Deutch, J.Chem.Phys. 62, 2130 (1975).

38 W.H.de Jeu, W.J.A.Goossens and P.Bordewijk, J.Chem.Phys. 61, 1985 (1974).

39 L.Benguigui, J. de Phys. 41, 341 (1980).

40 C.J.F.Bottcher and P.Bordewijk, Theory of electric polarization, Vol.2 (Elsevier Scientific Pub.Co., Amsterdam) 1978.

41 R.Shashidhar and K.V.Rao, Proc. Int. Liquid Crystals Conf., Bangalore, 1979, Ed. S. Chandrasekhar, (Heyden London, 1980) p.115.